Mechanical Aspects of Cardiac Performance

20

Michael K. Loushin, Jason L. Quill, and Paul A. Iaizzo

Abstract

This chapter is a review of commonly utilized monitoring techniques to assess the function of the general cardiovascular system. Specifically, means to assess arterial blood pressure, central venous pressure, pulmonary artery pressure, mixed venous oxygen saturation, cardiac output, pressure-volume loops, and Frank-Starling curves are described. Basic physiological principles underlying cardiac function are also briefly discussed.

Keywords

Cardiac pressure-volume loops • Blood pressure monitoring • Central venous pressure monitoring • Pulmonary artery pressure monitoring • Cardiac output • Cardiac index monitoring • Mixed venous saturation monitoring • Flow monitoring • Implantable monitoring

20.1 Introduction

This chapter is a review of commonly utilized monitoring techniques to assess the function of the general cardiovascular system. Specifically, means to assess arterial blood pressure, central venous pressure, pulmonary artery pressure, mixed venous oxygen saturation, cardiac output, pressure-volume loops, and Frank-Starling curves are described. Basic physiological principles underlying cardiac function are also briefly discussed.

Under normal physiologic conditions, the human heart functions as two separate pumps working in series; the right heart pumps blood through the pulmonary circulation and the left heart pumps blood through the systemic circulation. Each contraction of the heart and subsequent ejection of blood creates pressures that can be monitored clinically to assess the function of the heart and its work against resistance. In general, the mechanical function of the heart is described by the changes in pressure, volume, and flow that occur within each phase of the cardiac cycle, which is one complete sequence of myocardial contractions and relaxations.

20.2 Cardiac Cycle

The normal electrical and mechanical events of a single cardiac cycle of the left heart are correlated in Fig. 20.1. The mechanical events of the left ventricular pressure-volume curve are displayed in Fig. 20.2. During a single cardiac cycle, the atria and ventricles do not beat simultaneously; rather the atrial contraction occurs prior to ventricular contraction. This timing delay allows for proper filling of all four chambers of the heart. Recall that the left and right heart pumps function in series but contract simultaneously. The diastolic phase of the cardiac cycle begins with the opening

Electronic supplementary material: The online version of this chapter (doi:10.1007/978-3-319-19464-6_20) contains supplementary material, which is available to authorized users.

M.K. Loushin, MD (✉)
Department of Anesthesiology, University of Minnesota, MMC 294, 420 Delaware Street SE, Minneapolis, MN 55455, USA
e-mail: loush001@umn.edu

J.L. Quill, PhD
Medtronic, Inc., Minneapolis, MN, USA

P.A. Iaizzo, PhD
Department of Surgery, University of Minnesota, Minneapolis, MN, USA

P.A. Iaizzo (ed.), *Handbook of Cardiac Anatomy, Physiology, and Devices*, DOI 10.1007/978-3-319-19464-6_20

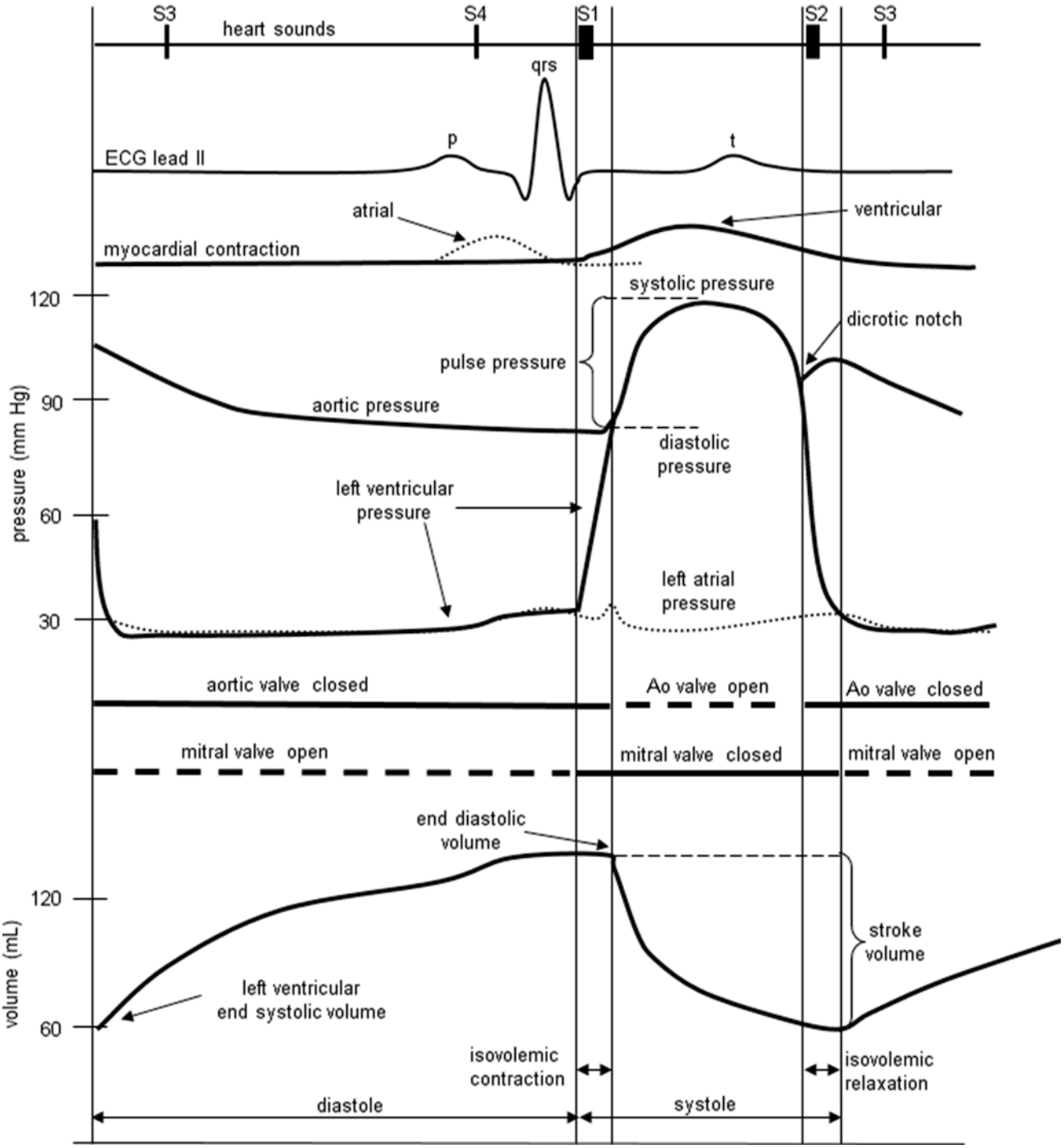

Fig. 20.1 Electrical and mechanical events of a single cardiac cycle within the left heart (see text for details)

of the tricuspid and mitral valves (atrioventricular valves). The atrioventricular valves open when the pressure in the ventricles falls below that in the atria. This can be observed in Fig. 20.1 for the left heart, in which the mitral valve opens when the left ventricular pressure falls below the left atrial pressure. At this moment, passive filling of the ventricle begins. In other words, blood that has accumulated in the atria behind the closed atrioventricular valves passes rapidly into the ventricles, and this causes an initial drop in atrial pressure. Later, pressure in all four chambers rises together as the atria and ventricles continue to passively fill in unison with blood returning to the heart through the veins (pulmonary veins to the left atrium and the superior and inferior vena cavae to the right atrium).

Contractions of the atria begin near the end of ventricular diastole, which is initiated by depolarization of the atrial

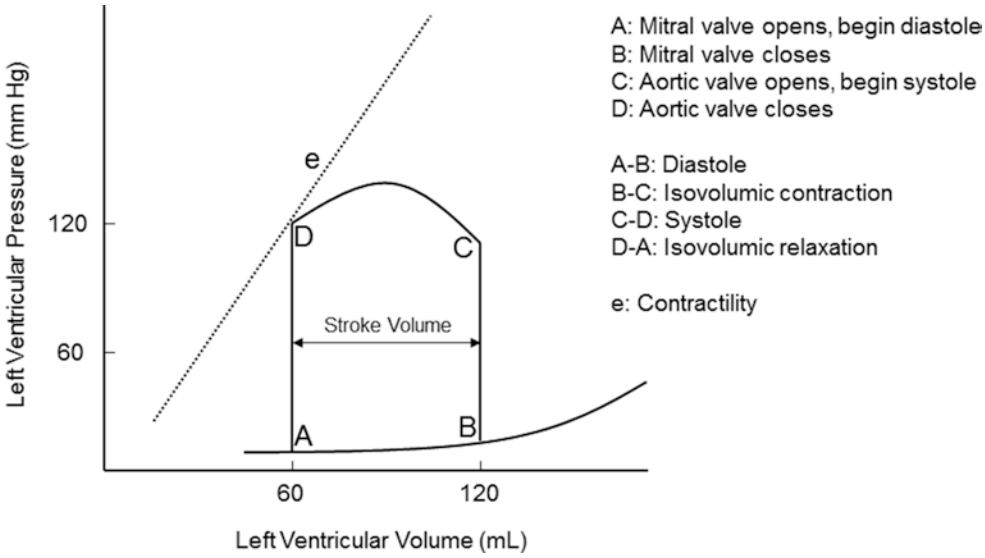

Fig. 20.2 Pressure-volume diagram of a single cardiac cycle (see text for details)

myocardial cells (sinoatrial node). Atrial depolarization is elicited at the P-wave of the electrocardiogram (Fig. 20.1, ECG lead II). The excitation and subsequent development of tension and shortening of atrial cells cause atrial pressures to rise. Active atrial contraction forces additional volumes of blood into the ventricles (often referred to as *atrial kick*). The atrial kick can contribute a significant volume of blood toward ventricular preload (approximately 20 %). At normal heart rates, the atrial contractions are considered essential for adequate ventricular filling. As the heart rate increases, atrial filling becomes increasingly important for ventricular filling because the time interval between contractions for passive filling becomes progressively shorter. Atrial fibrillation and/or asynchronized atrioventricular contractions can result in minimal contribution to preload, via the lack of a functional atrial contraction. Throughout diastole, atrial and ventricular pressures are nearly identical due to the open atrioventricular values which offer little or no resistance to blood flow. It should also be noted that contraction and movement of blood out of the atrial appendage (auricle) can be an additional source for increased blood volume.

Ventricular systole begins when the excitation passes from the right atrium, through the atrioventricular node, and through the remainder of the conduction system (His bundle and left and right bundle branches) to cause ventricular myocardial activation. This depolarization of ventricular cells underlies the QRS complex within the ECG (Fig. 20.1). As the ventricular cells contract, intraventricular pressures increase above those in the atria, and the atrioventricular valves abruptly close. Closure of the atrioventricular valves results in the first heart sound, S1 (Fig. 20.1). As pressures in the ventricles continue to rise together in a normally functioning heart, they eventually reach a critical threshold pressure at which the semilunar valves (pulmonary valve and aortic valve) open. The mechanical events of a single cardiac cycle and its pressure-volume relationship are displayed in Fig. 20.2. The normal time period between semilunar valve closures and atrioventricular valve openings is referred to as the *isovolumic contraction phase*. During this interval, the ventricles can be considered as closed chambers. Ventricular wall tension is greatest just prior to opening of the semilunar valves. Ventricular ejection begins when the semilunar valves open. In early left heart ejection, blood enters the aorta rapidly and causes the pressure within it to rise. Importantly, pressure builds simultaneously in both the left ventricle and the aorta as the ventricular myocardium continues to contract. This period is often referred to as the *rapid ejection phase*. A similar phenomenon occurs in the right heart; however, the pressures developed and those required to open the pulmonary valve are considerably lower, due to lower resistance within the pulmonary vascular system.

Pressures in the ventricles and outflow vessels (the aorta and pulmonary arteries) ultimately reach maximum peak systolic pressures. Under normal physiologic conditions, the contractile forces in the ventricles diminish after achieving peak systolic pressures. Throughout ejection, there are minimal pressure gradients across the semilunar valves due to their normally large annular diameters. Eventually the ventricular myocardium elicits minimal contraction to a point where intraventricular pressures fall below those in the outflow vessels. This fall in pressures causes the semilunar valves to close rapidly and is associated with the second heart sound, S2 (Fig. 20.1). A quick reversal in both aortic and pulmonary artery pressures is observed at this point, due to back pressure filling the semilunar valve leaflets. The back pressure on the valves causes the *incisura* or *dicrotic notch*, which can be detected by local pressure recording (e.g., with a locally placed Millar catheter). After complete closure of these valves, the intraventricular pressure falls rapidly and the ventricular myocardium relaxes. For a brief period, all four

cardiac valves are closed, which is commonly referred to as the *isovolumetric relaxation phase*. Eventually, intraventricular pressure falls below the rising atrial pressures, the atrioventricular valve opens, and a new cardiac cycle is initiated.

20.3 Cardiac Pressure-Volume Curves

Ventricular function can be analyzed and graphically displayed with a pressure-volume diagram. Both systolic and diastolic pressure-volume relationships during a single cardiac cycle are displayed in Fig. 20.2. Pressure-volume assessment of myocardial function on intact myocardium involves multiple factors such as preload, afterload, heart rate, and contractility. The area inside the pressure-volume loop is an estimate of the myocardial energy (work = pressure × volume) utilized for each stroke volume (stroke volume = end-diastolic volume − end-systolic volume). The shape of the normal pressure-volume loop changes with alterations in myocardial compliance, contractility, and valvular or myocardial disease.

Pressure-volume loops are displayed by plotting ventricular pressure (*y* axis) against ventricular volume (*x* axis) during a single cardiac cycle (Fig. 20.2). Points and segments along the pressure-volume loop correlate with specific mechanical events of the ventricle. The width of the pressure-volume loop is the stroke volume. Myocardial contractility is represented by the slope of the end-systolic pressure-volume relationship; this relationship defines the maximal pressure generated over time with a given myocardial contractility state. Contractility is proportional to change in pressure over time (dP/dt). The passive ventricular filling during diastole is defined by the end-diastolic pressure-volume relationship, and ventricular compliance is inversely proportional to the slope of the end-diastolic pressure-volume relationship. The effect of heart rate on the pressure-volume relationship cannot be assessed with a single pressure-volume loop. Instead, multiple pressure-volume loops must be obtained to assess effects of heart rate on the pressure-volume loop. By altering variables such as afterload, contractility, and/or preload, the mechanical events and pressure-volume relationship are displayed.

The pressure-volume diagram shows events of a single cardiac cycle (Fig. 20.2):

A: mitral valve opens; diastole begins.
B: mitral valve closes; diastole ends.
C: aortic valve opens; systole begins.
D: aortic valve closes; systole ends.
A-B: diastole, ventricular filling.
B-C: isovolumic contraction.
C-D: systole, ventricular ejection.
D-A: isovolumic relaxation.
e: contractility slope.

20.3.1 Preload

Preload is determined by the end-diastolic ventricular volume; it results from passive and active emptying of the atrium into the ventricle. Factors that affect this relationship, such as mitral stenosis and/or ventricular hypertrophy, will affect preload. The Frank-Starling curve also defines the relationship between preload and stroke volume; as end-diastolic volume increases, the stroke volume increases until the end-diastolic volume gets too excessive to allow proper ventricular contraction (Fig. 20.3). A pressure-volume loop is an alternative way to display the relationship between preload and stroke volume (Fig. 20.4); preload is the volume of blood in the ventricle at the end of diastole (point B in Fig. 20.4). An increase in preload is displayed by a right shift of the end-diastolic volume curve (A-B* in Fig. 20.4). In a normally functioning ventricle, an increase in preload while maintaining normal contractility and afterload results in increased stroke volume (SV* in Fig. 20.4). Excessive preload will not always result in increased stroke volume; excessive overdistention of the ventricle may result in heart failure (Fig. 20.5).

20.3.2 Contractility

Contractility is the relative ability of the myocardium to pump blood without changes in preload or afterload; it is influenced by intracellular calcium concentrations, the autonomic nervous system, humoral changes, and/or pharmacologic agents. A sudden increase in contractility with unchanged preload and afterload will result in increased stroke volume by ejecting more volume out of the ventricle (Fig. 20.6). The aortic valve opens at the same pressure and the ventricle ejects blood forward. Increased myocardial

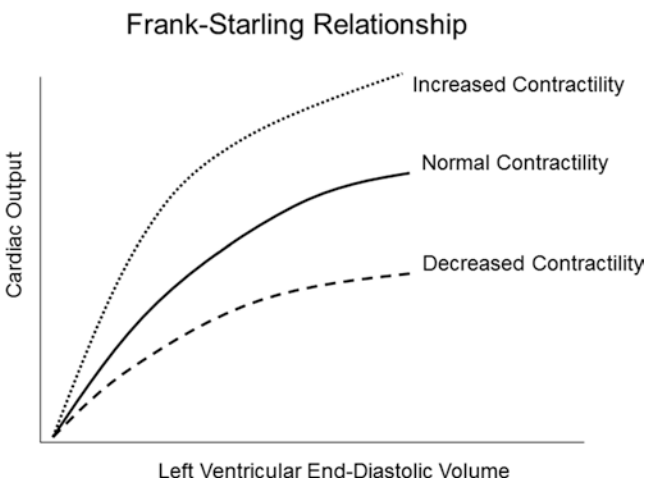

Fig. 20.3 The Frank-Starling relationship. As the end-diastolic volume increases, the cardiac output also increases. Excessive preload may eventually result in decreased cardiac output

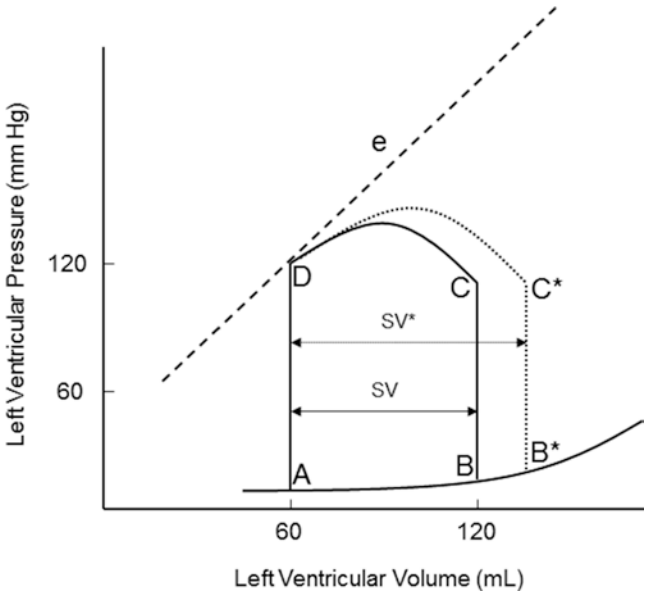

Fig. 20.4 Effect of acutely increased preload on the pressure-volume loop. Increasing preload while maintaining normal afterload and contractility results in increased stroke volume (*SV**). *e* contractility line, *SV* stroke volume

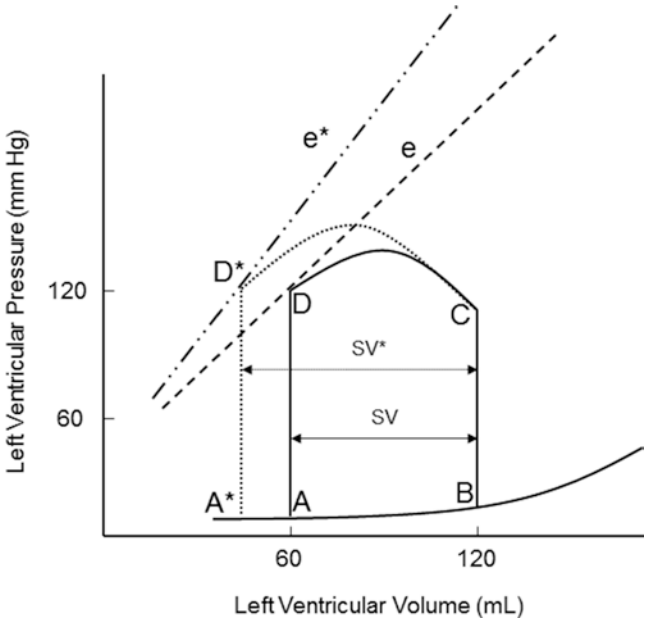

Fig. 20.6 Effects of acutely increasing contractility on the pressure-volume loop. Increasing contractility while maintaining normal preload and afterload results in increased stroke volume (*SV**). Note the increased slope of the contractility line (*e**). The area of loop D* is larger, indicating greater myocardial work per stroke volume. *e* and *e** contractility lines, *SV* stroke volume

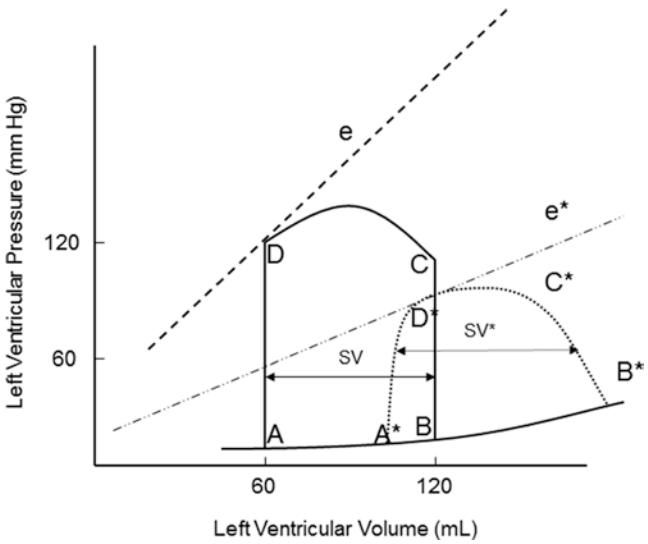

Fig. 20.5 Effect of ventricular failure on the pressure-volume loop. In heart failure, the myocardium compensates its inability to contract by increasing preload in an attempt to maintain stroke volume. Excessive preload eventually leads to worsening of heart failure. *e* and *e** contractility lines, *SV* stroke volume

contractility forces more blood out of the ventricle during systole, which is displayed by a lower end-systolic volume. Note the change in SV* (Fig. 20.6) with increased contractility; the end-systolic volume is lower due to increased contractility resulting in increased stroke volume. With increased myocardial contractility and unchanged preload, the resulting pressure-volume loop shifts to the left, maintaining normal stroke volume**.** An increase in contractility is graphically displayed by the increase in the slope of line e* in Fig. 20.6. During ejection, the myocardium contracts from C to D* (Fig. 20.6). During conditions of lower end-diastolic volume, a normal stroke volume may be maintained by increasing contractility. Inotropes such as dopamine and epinephrine will increase contractility, which assists in maintaining adequate stroke volume during low contractility states such as heart failure and/or cardiogenic shock.

In heart failure, the myocardium has decreased capacity to pump blood and maintain normal cardiac output. Heart failure may be acute (e.g., acute myocardial infarction, acute cardiogenic shock, or fluid overload) or it may be chronic (e.g., chronic congestive heart failure). In progressive heart failure, the myocardium often compensates its inability to contract by increasing preload and decreasing afterload in an attempt to maintain stroke volume (Fig. 20.5).

The increase in preload moves the myocardium up the Frank-Starling curve such that, by increasing end-diastolic volume, normal stroke volume may be maintained. The increase in preload and worsening heart failure eventually leads to ventricular dilatation and venous congestion. During heart failure, sympathetic tone increases as levels of circulating norepinephrine and epinephrine attempt to maintain normal cardiac output by increasing contractility and heart rate. The body's compensatory mechanism for heart failure may eventually become counterproductive and thus even worsen the situation.

20.3.3 Afterload

Afterload is another vital factor relative to stroke volume and therefore blood pressure. Afterload is most often equated with ventricular wall tension, which is also considered as the pressure the ventricle must overcome to eject a volume of blood past the aortic valve. In most normal clinical situations, afterload is assumed to be proportional to systemic vascular resistance. Wall tension is greatest at the moment just before opening of the aortic valve and can be described by LaPlace's law:

$$\text{Circumferential stress} = \text{Pr}/\,2H$$

where circumferential stress = wall tension, P = intraventricular pressure, r = ventricular radius, and H = wall thickness.

An increase in afterload requires ventricular pressure to increase during isovolumic contraction before the aortic valve opens (Fig. 20.7). Due to the increase in afterload, the ability of the ventricle to eject blood is decreased. This results in decreased stroke volume (SV* in Fig. 20.7a) and increased end-systolic volume (B* in Fig. 20.7b). If afterload remains increased, the myocardium establishes a new steady state that is shifted to the right and stroke volume is restored. A patient with severe aortic stenosis will likely elicit a pressure-volume loop as in Fig. 20.7. The myocardium usually compensates by increasing contractility to maintain adequate stroke volume. Thus, patients with hemodynamically significant aortic stenosis often develop left ventricular hypertrophy.

Afterload may be inversely related to cardiac output. In a dysfunctional myocardium, such as congestive heart failure, stroke volume decreases with increases in afterload. Importantly, increase in afterload also requires the myocardium to expend more energy to eject blood during systole. Conditions such as supravalvular or infravalvular stenoses or obstructions can also impact afterload or wall tension. A clinical example is idiopathic hypertrophic subaortic stenosis (IHSS), a heart condition characterized by significant hypertrophy of the left ventricle and interventricular septum. In turn, the hypertrophied muscle can then obstruct left ventricular outflow of blood during systole, increasing afterload and wall tension.

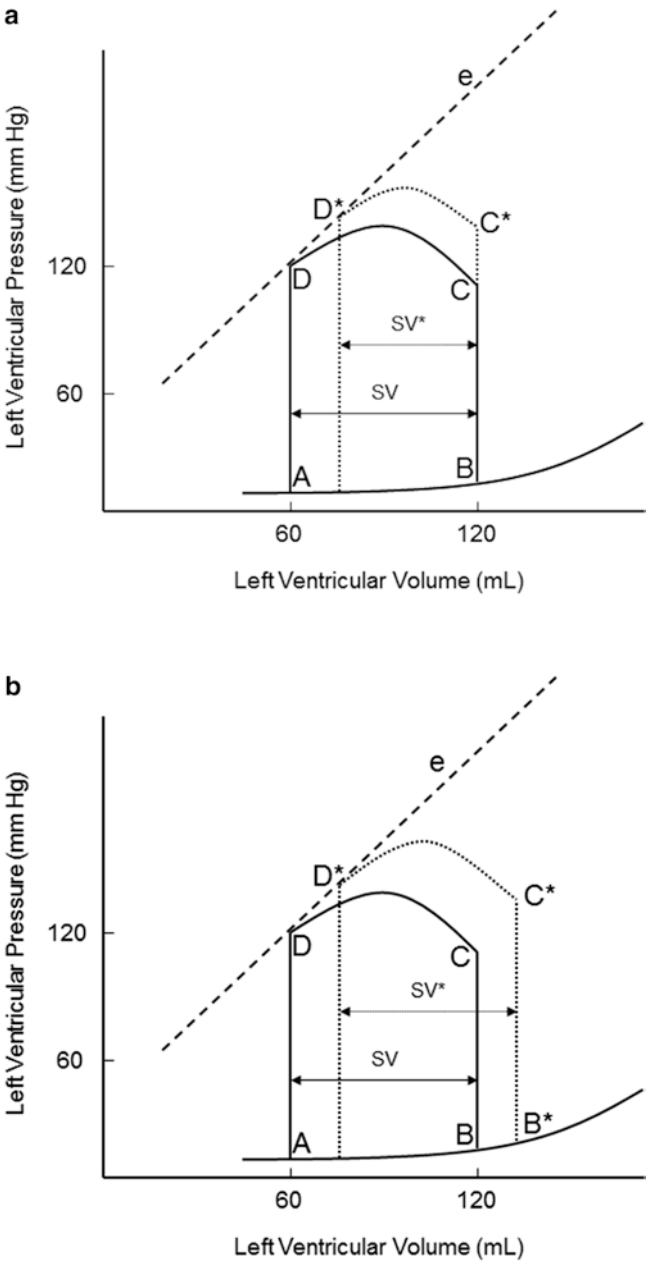

Fig. 20.7 (**a**) Effects of acutely increasing afterload on the pressure-volume loop. An increase in afterload, while maintaining normal contractility and preload, results in decreased stroke volume (*SV**). A higher pressure is also required before the aortic valve opens (*C**). (**b**) Restoration of stroke volume after increasing afterload. An increase in afterload, while maintaining normal contractility and preload, results in decreased stroke volume (*SV**). A higher pressure is also required before the aortic valve opens (*C**). *e* contractility line, *SV* stroke volume

20.3.4 Sonomicrometry Crystals

A common method for obtaining pressure-volume loops, and the changes observed by varying preload, afterload, or contractility, is to use sonomicrometry crystals for volume measurements in combination with a pressure-sensing catheter placed in the left ventricle. Sonomicrometry consists of piezoelectric crystals that transmit ultrasound signals through tissue to other crystals, where the signal is received; a distance measurement between two given crystals can be determined based upon the travel time of the ultrasound signal and the fiber orientation of the tissue. The piezoelectric (sonomicrometry) crystals function omnidirectionally and act as both receiver and transmitter with as many as 32 peers (in most commonly available systems). Complex, moving

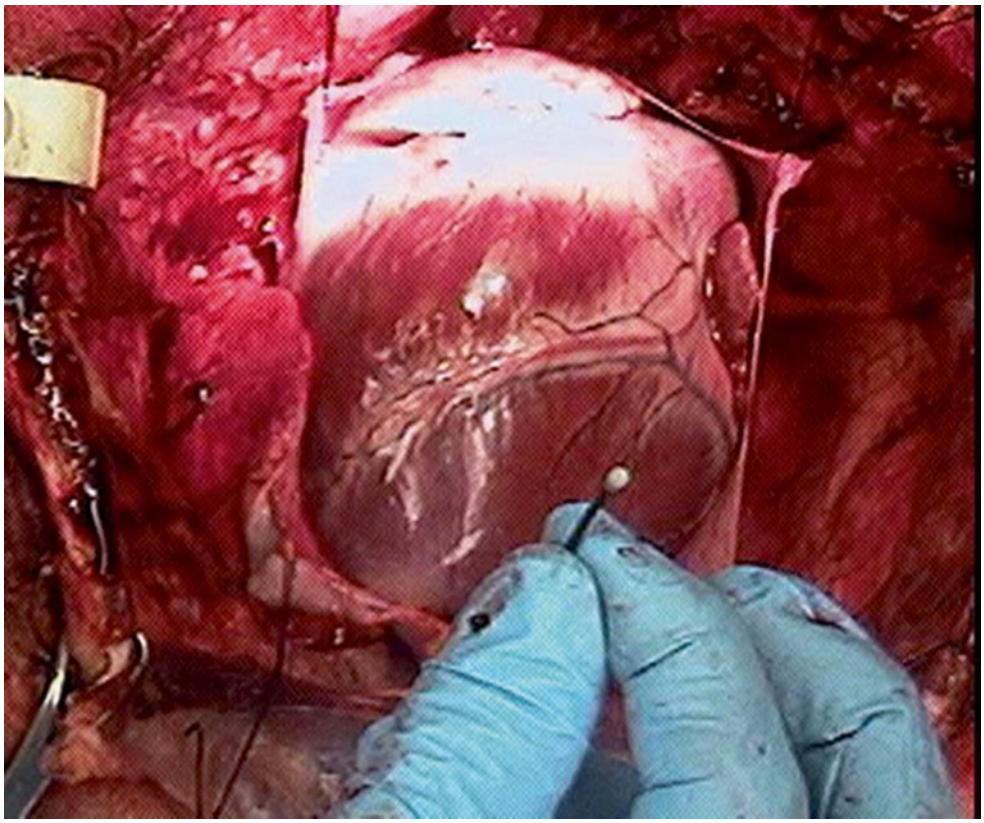

Fig. 20.8 A common sonomicrometry crystal placement. The crystal is shown prior to transmural implantation in a swine heart

3D geometries can then be modeled using techniques like sonomicrometry array localization. A sonomicrometry crystal can be seen in Fig. 20.8, where it is held in preparation for insertion through the epicardium.

Placement of four sonomicrometry crystals transmurally within the left ventricle, as well as the resulting pressure-volume loops, can be viewed online (Online Videos 20.1 and 20.2). The method shown in these supplemental videos places four sonomicrometry crystals—one on the anterior surface, the second on the posterior surface, a third crystal at the base of the left ventricle (superior), and a final crystal at the left ventricular apex (inferior). The placement of the crystals in this pattern creates two distance measurements (anterior-posterior and base-apex) that are measured continuously through the cardiac cycle. By assuming the left ventricle is the shape of an ellipsoid, changes in volume can be continuously estimated.

Traditionally, sonomicrometry has been used to determine cardiac function relative to large research animals (dogs, pigs, sheep, etc.). Both in vivo and in vitro studies can be performed which elucidate global cardiac function under a variety of conditions. Understanding the velocity of ultrasound through tissue is critical to acquiring accurate dimensions in a sonomicrometry system. The velocity of ultrasound is affected by a variety of factors including muscle fiber direction and composition, as well as the contractile state. In most biological tissues, the velocity of sound is approximately 1540 m/s.

A sonomicrometry system can use as few as two transducers but typically employs between six and thirty-two transducers. Transducers are the piezoelectric crystals which are attached to electronics consisting of a pulse generator and a receiver. Distance is measured by energizing the transmitter with a train of high-voltage spikes or square waves (both less than a microsecond in duration) to produce ultrasound. This excites the piezoelectric crystal to begin oscillating at its resonant frequency. This vibratory energy propagates through the medium and eventually comes in contact with piezoelectric crystals acting as receivers. These crystals begin vibrating and generate signals on the order of one millivolt. The piezoelectric signals are amplified and the distances between pairs of crystals are calculated. By monitoring the difference in time from transmission to reception of such signals and knowing the speed of sound through the particular medium, the intercrystal distances can be calculated. With current systems, these computations take less than 1 ms.

In addition to sonomicrometry crystals being used in the manner described, several other types of studies have found sonomicrometry measurements to be helpful. Regional studies have been performed that focus on specific areas of the heart, investigating regional timing and left ventricular shortening [1]. The advent of three-dimensional sonomicrometry,

or *sonomicrometry array localization*, has made possible the detailed study of discrete anatomical points throughout the cardiac cycle [2, 3]. A volume of data now exists describing the motion of valves, papillary muscles, ventricles, and atria. Another application involves tracking mobile components through the heart such as cardiac catheters [4]. We believe that these applications of sonomicrometry are important enough to be described in detail below.

In sonomicrometry array localization, the 3D position of each crystal is calculated from multiple intertransducer distances. This is done using a statistical technique called *multidimensional scaling*; such assessment gives the experimenter the ability to take the scalar sonomicrometer measurements and generate 3D geometry. Multidimensional scaling generates 3D coordinates for each crystal from a group of chord lengths in the array. By starting with an initial coordinate estimate and applying the Pythagorean theorem, a matrix of estimated distances is generated which corresponds to the actual measured distances. Using an iterative approach, multidimensional scaling then optimizes the value for the distance calculation by minimizing what is called the *stress function*. If the distances measured between crystals are exact (no measurement error), then one solution with zero stress exists, which represents the intercrystal distances exactly. As measurement error increases, a zero solution to the stress function becomes impossible and the iterations begin seeking a minimum value. The globally minimum stress point defines the optimum 3D configuration. A similar style is used to generate an estimate of the error associated with each distance. The result of this analysis is a 3D moving model with an average error of approximately 2 mm. The advent and description of the feasibility assessment of this technique is described in detail by Ratcliffe et al. [2] and Gorman et al. [3].

The first reported application of this technology described the 3D modeling of the ovine left ventricle and mitral valve. The study involved a 16-transducer array in which three transducers were sutured to the chest wall and the remaining thirteen were placed both epicardially and endocardially on the ventricular wall, the papillary muscles, and the mitral valve. The three crystals attached to the chest wall provided a fixed coordinate system from which whole-body motion could be differentiated from cardiac motion. This study produced 3D depictions of the shape of the mitral annulus throughout the cardiac cycle, as well as quantitative images of ventricular torsion. Such applications open up many possibilities relative to chronic studies focusing on ventricular remodeling following trauma like myocardial infarction.

Another interesting application of sonomicrometry, available due to the development of sonomicrometry array localization, is the cardiac catheter tracking described by Meyer et al. [4]. The system involves placing seven sonomicrometric crystals in the epicardium of an ovine heart and tracking the position of a catheter anywhere from one to five attached crystals. In this system, average distance errors on the order of 1.0 mm were demonstrated by Meyer et al. The clinically relevant endpoint for this tool would be to replace the epicardial transceivers with transceivers mounted in catheters and deployed endocardially in a minimally invasive manner.

20.3.5 Conductance Catheter

Conductance catheters offer an alternative method for obtaining pressure-volume loops. In this method, a catheter is typically equipped with eight electrodes and a pressure lumen. The conductance catheter is placed retrograde across the aortic valve, so that the first electrode is positioned in the left ventricular apex and the eighth electrode is positioned across the aortic valve (Fig. 20.9). The pressure lumen is located within the left ventricle, usually at the distal tip of the conductance catheter.

The outermost electrodes of the conductance catheter produce an electric field, with the remaining electrodes sensing differentials in voltage potential. The use of conductance to measure volume arises from the fact that blood is a good conductor relative to the surrounding myocardium (160 vs.

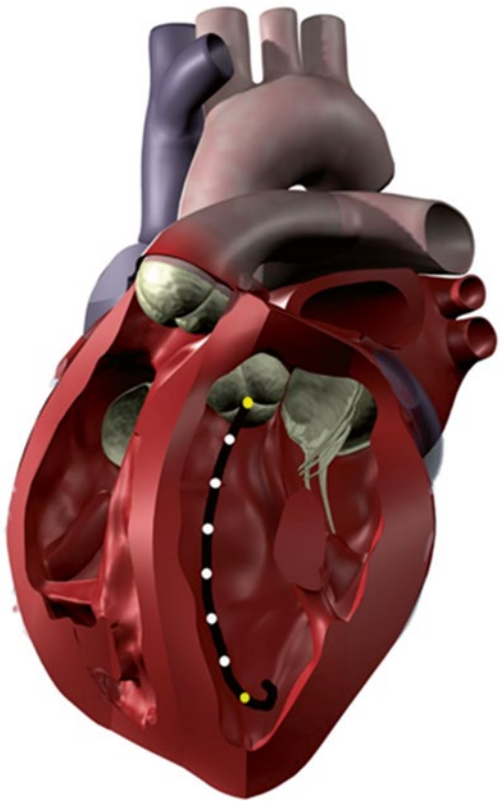

Fig. 20.9 When properly placed within the left ventricle, a conductance catheter spans from the apex to the aortic valve. The outermost electrodes (*yellow*) produce an electric field, and the inner electrodes (*white*) measure voltage differences that are related to volume changes within the chamber. A pressure sensor is typically incorporated into the distal tip of the catheter

400 Ω cm) [5]. When the ventricle is in diastole and filled with blood, the conductivity of the chamber will be much higher than during systole. The volume of the heart chamber is then analyzed as a series of conductive cylinders stacked upon each other, with a height predetermined as the distance between the electrodes. A change in the cross-sectional area of one of these cylinders is synonymous with a decrease in blood volume and a change in resistance, which is measured by the sensing electrodes.

The left ventricular volume can then be calculated as a voltage varying with time ($V(t)$), based upon the distance between the electrodes (L), the specific conductivity of blood (σ), the sum of the conductances that vary with time ($G(t)$), a dimensionless constant (α), and a correction term (C) [6]:

$$V(t) = \frac{L^2}{\alpha\sigma} G(t) - C$$

The conductance catheter was developed in the early 1980s by Baan et al. [6]. This method has shown reliable left ventricular segmental volumes when compared to cine-CT scans [7] and sonomicrometry crystals. Additionally, the conductance methods could be optimally suited for right ventricular pressure-volume curves [8]. Sonomicrometry methods and angiography require the assumption of an ellipsoid shape for left ventricular measurements; the complex geometric shape of the right ventricle makes these methods ill suited for volume measurements on the right side of the heart.

Both sonomicrometry crystals and conductance catheters are proven techniques for the measurement of left ventricular and aortic root volumes [9]. These technologies are applicable to many different study designs, yet care should be taken to choose the best method based upon the needs of the study. For studies involving complex geometric shapes, a conductance catheter may be the easiest method to obtain absolute volume changes, but a technique such as sonomicrometry array localization may be advantageous if the relative motion of geometric components is of interest.

20.4 Blood Pressure Monitoring

The cardiovascular system is most commonly assessed by monitoring arterial blood pressure. Blood pressure is proportional to the product of cardiac output and systemic vascular resistance:

$$\mathrm{BP} = \mathrm{CO} \times \mathrm{SVR}$$

$$\mathrm{CO} = \mathrm{HR} \times \mathrm{SV}$$

$$\mathrm{MAP} = 1/3\,\mathrm{SBP} + 2/3\,\mathrm{DBP}$$

where BP = blood pressure, CO = cardiac output, SVR = systemic vascular resistance, HR = heart rate, SV = stroke volume, MAP = mean arterial pressure, SBP = systolic blood pressure, and DBP = diastolic blood pressure. Stroke volume is dependent upon preload, afterload, and contractility (Fig. 20.10).

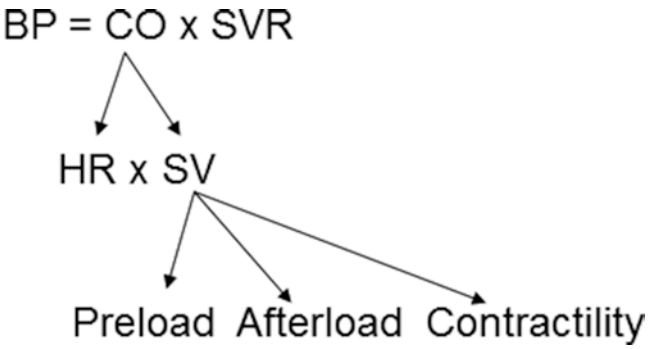

Fig. 20.10 Blood pressure monitoring which is proportional to the product of cardiac output and systemic vascular resistance. *BP* blood pressure, *CO* cardiac output, *HR* heart rate, *SV* stroke volume, *SVR* systemic vascular resistance

Blood pressure can be defined to consist of three components: systolic blood pressure, mean arterial pressure, and diastolic blood pressure. Systolic blood pressure is the peak pressure during ventricular systole, mean arterial pressure is a crucial determinant for adequate perfusion of other major organs, and diastolic blood pressure is the main determinant for myocardial perfusion. Recall that the majority of coronary blood flow occurs during diastole.

Commonly, arterial blood pressure monitoring involves two primary techniques—noninvasive (indirect) and invasive (direct) methods. The decision to utilize either blood pressure monitoring method depends on multiple factors such as: (1) level of a patient's cardiovascular stability, (2) perceived need for frequent arterial blood samples, (3) relative frequency of blood pressure recordings, and/or (4) type of major surgery or trauma the patient will undergo. One of the advantages of an invasive blood pressure monitor is that it provides continuous, beat-to-beat blood pressures (Online JPG 20.1). Typically, direct arterial blood pressure monitoring is considered to be required when a cardiopulmonary bypass machine is utilized during cardiac surgery. Since there is no pulsatile flow during such surgery, the noninvasive methods to monitor blood pressure cannot be employed. Also, patients with a ventricular assist device may require an invasive arterial monitor, as the noninvasive technique may not provide accurate systemic blood pressures (for more information on ventricular assist devices, see Chap. 39).

20.4.1 Noninvasive Arterial Blood Pressure Monitoring

Noninvasive blood pressure assessment is the most utilized and simplest technique to monitor arterial blood pressure. This technique utilizes a blood pressure cuff and the principle

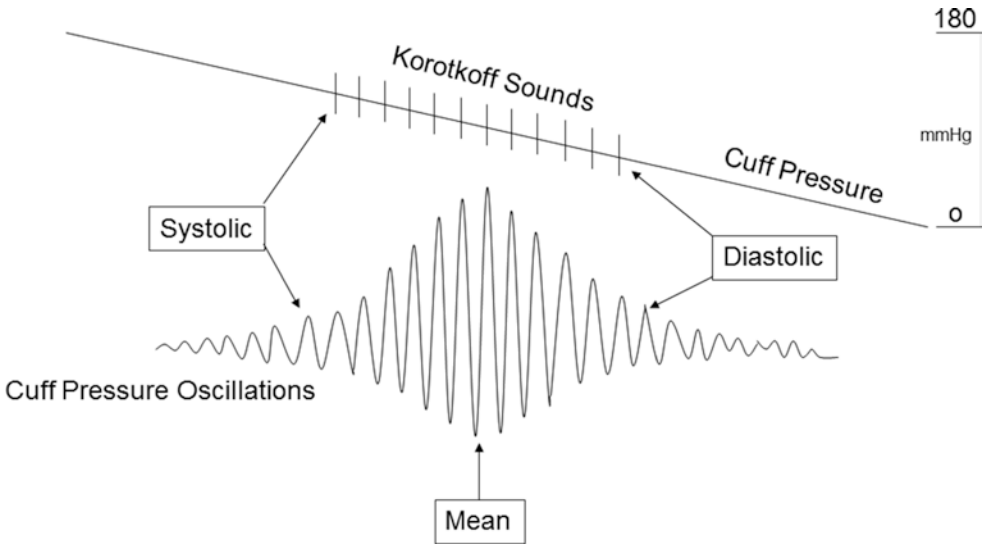

Fig. 20.11 An example of noninvasive blood pressure monitoring. As blood flow is restored with release of the blood pressure cuff, the arterial wave oscillations increase. The increase in oscillation amplitudes is associated with systolic blood pressure and presence of Korotkoff sounds. The peak of oscillations is associated with mean arterial pressure. Return of oscillations to baseline is diastolic blood pressure and end of Korotkoff sounds

of pulsatile flow. A blood pressure cuff is applied to a limb such as forearm or leg and is inflated to a pressure greater than systolic blood pressure, which stops blood flow distal to the inflated cuff. As the pressure in the cuff is gradually decreased, blood flow through the artery is restored. The change in arterial pressure and blood flow creates oscillations which can be detected by auscultation of Korotkoff sounds and oscillometric methods. For accurate blood pressure measurement, the width of the cuff should be approximately one-third the circumference of the limb. A small, improperly sized cuff will overestimate systolic blood pressure, while a large cuff will underestimate the pressure. The rate of cuff deflation should be slow enough to hear Korotkoff sounds or detect oscillations. Noninvasive blood pressure monitors do not work if there is no pulsatile flow.

The automated method of noninvasive blood pressure monitoring is the *oscillometric* technique. Most oscillometric blood pressure monitors have oscillotonometers and a microprocessor. The blood pressure cuff is inflated until no oscillation is detected. As the cuff pressure is decreased, flow in the distal blood vessel is restored and amplitude of oscillations increases. A large increase in arterial wave oscillation amplitude is recorded as systolic blood pressure, the peak oscillation as mean arterial pressure, and the sudden decrease in amplitude as diastolic blood pressure (Fig. 20.11). Due to the sensitivity of the monitoring system, the mean arterial pressure is usually the most accurate and reproducible. For more details on such monitoring, refer to Chap. 18.

20.4.2 Invasive Arterial Blood Pressure Monitoring

Continuous blood pressure monitoring is best accomplished by direct intra-arterial blood pressure monitoring. Direct pressure monitoring allows for continuous beat-to-beat monitoring of arterial pressure, and the recorded arterial waveform provides temporal information relative to cardiovascular function. Direct pressure monitoring is often employed in clinical settings such as: (1) during major trauma and vascular surgery, (2) in patients with sepsis, (3) during cardiopulmonary bypass where there is no pulsatile flow, (4) in patients with significant cardiovascular instability or fluctuations, and (5) in patients requiring tight blood pressure control, such as hypotension. Further, patients with significant cardiopulmonary disease (i.e., those in an intensive care unit) may require invasive arterial blood pressure monitoring (Table 20.1).

Table 20.1 Accepted indications for direct arterial blood pressure monitor

Major surgery
Major trauma
Major vascular (i.e., carotid endarterectomy, aortic aneurysm)
Cardiopulmonary bypass surgery
Myocardial dysfunction (i.e., myocardial ischemia/infarct, heart failure, dysrhythmias)
Uncontrolled/labile blood pressure (i.e., hypertension, hypotension)
Inaccurate noninvasive monitor (i.e., morbid obesity)
Sepsis/shock
Pulmonary dysfunction

Besides providing blood pressure assessment, the arterial waveform also presents information about cardiovascular function. For example, the upstroke of an arterial waveform correlates with myocardial contractility (dP/dT), while the downstroke gives information relative to peripheral vascular resistance. The position of the dicrotic notch gives insights as to the systemic vascular resistance; a low dicrotic notch position on the arterial waveform may infer low vascular resistance, while a high dicrotic notch usually relates to higher systemic vascular resistance. Furthermore, by integrating the area under the curve of the arterial waveform, the stroke volume may also be estimated.

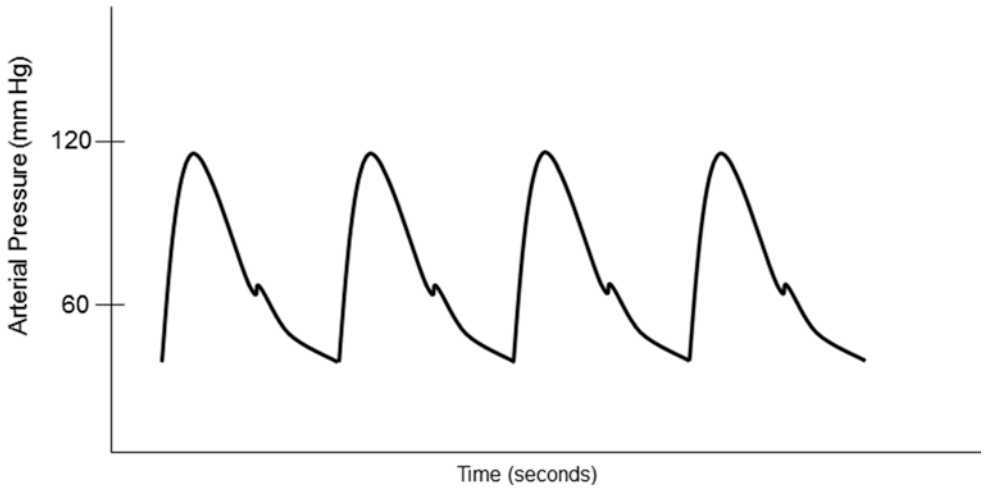

Fig. 20.12 An example of an arterial blood pressure wave from a typical optimally damped arterial blood pressure waveform. The peak portion of the waveform corresponds to the systolic blood pressure and the trough corresponds with the diastolic blood pressure. The dicrotic notch is associated with closing of the aortic valve. Information about cardiovascular function can be estimated from the waveform. The upstroke correlates with myocardial contractility. The downstroke and position of the dicrotic notch give information about systemic vascular resistance. The stroke volume is estimated by integrating the area under the curve

Direct arterial blood pressure monitoring typically involves cannulation of a peripheral artery and transducing the pressure (Online JPGs 20.2 and 20.3). An indwelling arterial catheter is connected to pressure tubing containing saline, which is then connected to a pressure transducer and monitoring system. Typical transducers contain strain gauges (stretch wires or silicon crystals) that distort with changes in blood pressure. The strain gauges contain a variable resistance transducer and a diaphragm which links the fluid wave to electrical signals. When the transducer diaphragm is distorted, there is a change in voltage across resistors of a Wheatstone bridge circuit (Online JPG 20.4). The transducer is constructed using a circuit so that voltage output can be calibrated proportional to the blood pressure. Standard pressure transducers are calibrated to 5 μV per volt excitation per mmHg [10]. Commonly, the electrical signals from such pressure monitoring systems are filtered, amplified, and displayed on a monitor, thus providing a typical arterial pressure waveform. It is important that the arterial pressure transducer be positioned and calibrated accurately at the level of the heart. Improper transducer height will result in inaccurate blood pressures; if the pressure transducer is positioned too high, the blood pressure is underestimated, while a lower positioned transducer will overestimate the actual blood pressure.

Common sites for intra-arterial cannulation for arterial pressure monitoring are the radial, brachial, axillary, or femoral arteries. Although the ascending aorta is the ideal place to monitor central arterial pressure waveforms, this is not practical in most clinical settings. However, it should be noted that pressure measurements in the more peripheral arteries become distorted when compared to central aortic pressure waveform (Fig. 20.12). Peripherally, the systolic blood pressure may be higher and diastolic blood pressure lower, while the mean

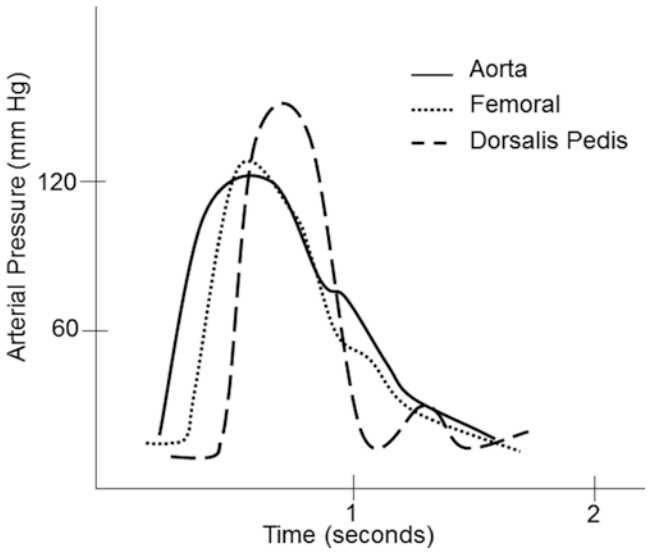

Fig. 20.13 A typical example of an arterial pressure waveform recorded from the ascending aorta. As the pressure monitoring site is moved more peripherally, the morphology of the waveform changes due to changes in arterial wall compliance as well as oscillation and reflection of the arterial pressure wave. Notice in the dorsalis pedis arterial waveform the absence of the dicrotic notch, overestimation of systolic blood pressure, and underestimation of diastolic pressure. Also note the presence of a small reflection wave

arterial pressure is usually similar to central aortic pressure. The pressure waveform becomes more distorted as pressure is measured farther away from the aorta. This distortion is due to a decrease in arterial compliance and reflection and oscillation of the blood pressure waves. For example, an arterial pressure wave monitored from the dorsalis pedis will be significantly different from a central aortic wave when it is graphically displayed (Fig. 20.13). There is also a loss in

amplitude or absence of the dicrotic notch, an increase in systolic blood pressure, and a decrease in diastolic blood pressure. One should also be aware of the possible appearance of a reflection wave as the blood pressure is monitored from a peripheral site. Importantly, risks associated with indwelling intra-arterial pressure catheter include thrombosis, emboli, infection, nerve injury, and hematoma.

20.4.3 Pressure Transducer System

In clinical settings, arterial and venous blood pressures and waveforms are displayed by utilization of a pressure transducer monitoring system. A typical system includes: (1) an indwelling intravascular catheter, (2) pressure tubing, (3) a pressure transducer, (4) stopcock and flush valve, (5) a high-pressure fluid bag, and (6) a graphical display monitor and microprocessor (Figs. 20.14a, b).

The pressure wave derived from the transducer system is a summation of sine waves at different frequencies and amplitudes. The fundamental frequency (first harmonic) is equal to the heart rate. Therefore, at a heart rate of 120 beats per minute, the fundamental frequency is 2 Hz. Since the first ten harmonics of the fundamental frequency make significant contributions to the arterial waveform [11], frequencies up to 20 Hz make major contributions to the pressure waveform. It is generally considered for most recording systems that the maximum significant frequency in the arterial blood pressure signal is approximately 20 Hz [12].

All materials have a natural frequency, also known as *resonant frequency*. The natural frequency of the monitoring system is the frequency at which the pressure monitoring system resonates and amplifies the actual blood pressure signal [12, 13]. If the natural frequency of the system is near the fundamental frequency, the blood pressure waveform will be amplified, giving an inaccurate pressure recording. The natural frequency is defined by the following equation [14]:

$$\mathrm{fn} = \left(d / 8\right) * \left(3 / \pi L \rho V_{\mathrm{d}}\right)^{1/2}$$

$$\varsigma = \left(16n / d^{3}\right) * \left(3LV_{\mathrm{d}} / \pi\rho\right)^{1/2} \left(\text{damping coefficient}\right)$$

where fn = natural frequency, d = tubing diameter, n = viscosity of fluid, L = tubing length, ρ = density of fluid, and V_{d} = transducer fluid volume displacement

In order to increase accuracy of the blood pressure waveform, the natural frequency needs to be increased while the amount of distortion is reduced. The optimal natural frequency should be at least 10 times the fundamental frequency, which is then greater than the tenth harmonic of the fundamental frequency [11, 12]. Therefore, the natural frequency should be greater than 20 Hz. In clinical settings, the input frequency is usually close to the monitoring system's natural frequency, which ranges from 10–20 Hz. When the input frequency is close to the natural frequency, the system amplifies the actual pressure signal. Ideally, the natural frequency should exceed the maximum significant frequency in a blood pressure signal which is about 20 Hz [12]. An amplified system typically requires damping to minimize distortion; an underdamped system will result in amplification, while an overdamped system will result in reduced amplification.

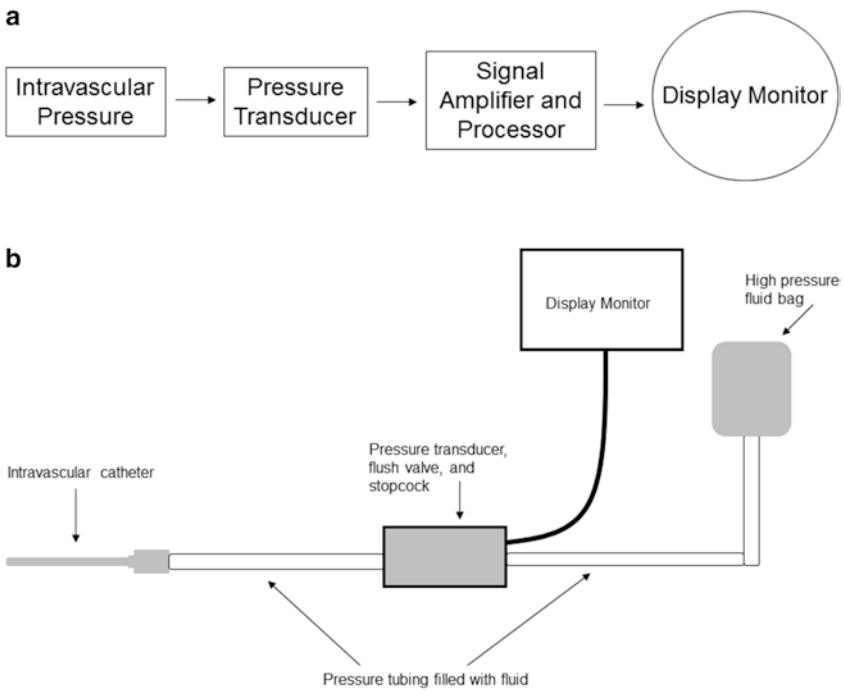

Fig. 20.14 Schematics of a pressure transducer monitoring system (see text for details)

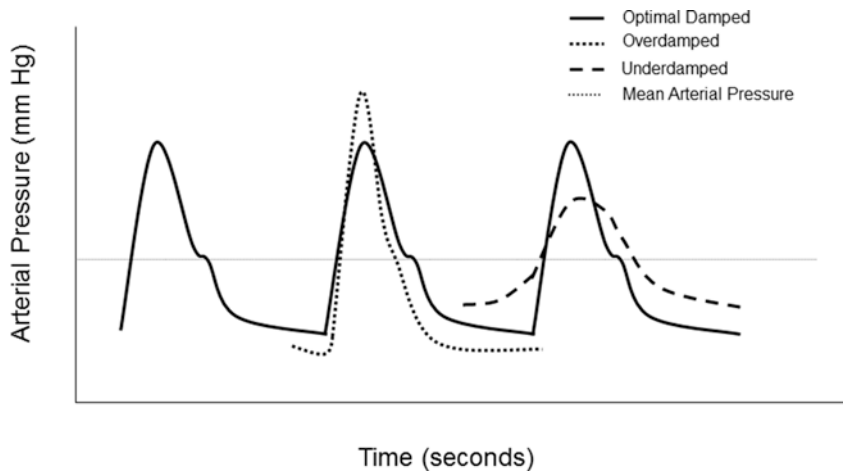

Fig. 20.15 Effects of damping on the arterial pressure waveform. In an underdamped pressure monitoring system, the pressure wave overestimates the systolic blood pressure and underestimates the diastolic blood pressure. In an overdamped system, the pressure wave underestimates the systolic blood pressure and overestimates the diastolic blood pressure. The mean arterial pressure remains essentially unchanged

The ability of the system to extinguish oscillations through viscous and frictional forces is the damping coefficient (ς) [15]. Some degree of damping may be required to prevent overamplification of blood pressure waveforms. It is considered that more damping is required especially in patients with higher heart rates, such as neonates. At higher heart rates, the tenth harmonic of the fundamental frequency will approach the natural frequency and the waveform is amplified. Overamplification, or ringing, can be adjusted by increasing the damping coefficient. Specifically, in an overamplified system, a connector with an air bubble can intentionally be placed in line with the pressure transducer; the air bubble damps the system to diminish ringing.

The accuracy of pressure transducers is considered optimal in the following situations: low compliance of the pressure catheter and tubing, low density of fluid in the pressure tubing, and short tubing with a minimal number of connectors. Note that a suboptimal pressure system may produce an underdamped or overdamped pressure waveform; an underdamped waveform will overestimate systolic blood pressure, while an overdamped waveform will underestimate systolic blood pressure. Damping occurs when factors such as compliance of tubing, air bubbles, and blood clots decrease the peaks and troughs of the pressure sine waves by absorbing energy and diminishing the waveform. In an underdamped system, the pressure waves generate additive harmonics, which may also lead to an overestimated blood pressure. In an overdamped system, a pressure wave may be impeded from adequately propagating forward. Overdamping may occur due to air bubbles in the pressure lines, kinks, blood clots, low-flush bag pressures, and multiple stopcocks or injection ports. This often results in underestimation of systolic blood pressure and overestimation of diastolic blood pressure. Fortunately, the mean arterial pressure is minimally affected by dampening (Fig. 20.15).

Optimal pressure waveforms can be obtained when there is balance between the degree of damping and distortion from the pressure tubing system. A simple way to assess damping is to observe the results from a high-pressure fluid flush. In the flush test, the pressure transducer system is flushed and the resulting oscillations (ringing) are observed. In an optimally damped system, a baseline results after one oscillation (Fig. 20.16). In an overdamped system, the baseline is reached without oscillations and the waveform is blunted. In an underdamped system, the flush test results in multiple oscillations before the waveform reaches baseline.

20.4.4 Transducer Catheters

Common clinical methods to monitor arterial and venous pressures utilize a pressure transducer system that requires a fluid-filled system. Transducer catheters such as Millar catheters (Online JPG 20.5) monitor pressures directly from a sensor incorporated within the tip of the catheter. A sensor (Online JPG 20.6) placed directly at the end of the catheter allows direct and constant measurement of pressures, thus eliminating the intrinsic inaccuracies of a fluid-filled system.

In general, transducer catheters are more accurate than conventional fluid-filled systems. Motion artifact is nearly eliminated and the issues of overdamped and underdamped systems are not present. Accurate pressure readings can be obtained with the catheter at any height; readings are not affected by the height of the pressure transducer as in the conventional system. With transducer catheters, there is no time delay since pressure is monitored directly at the source. Compared to the conventional fluid system, transducer catheters have high inherent fidelity (>10 MHz).

20.5 Central Venous Pressure Monitoring

An estimate of intravascular volume status and right heart function can be assessed with a central venous pressure catheter. Central venous pressure is ideally considered as the mean venous blood pressure at the junction of the right

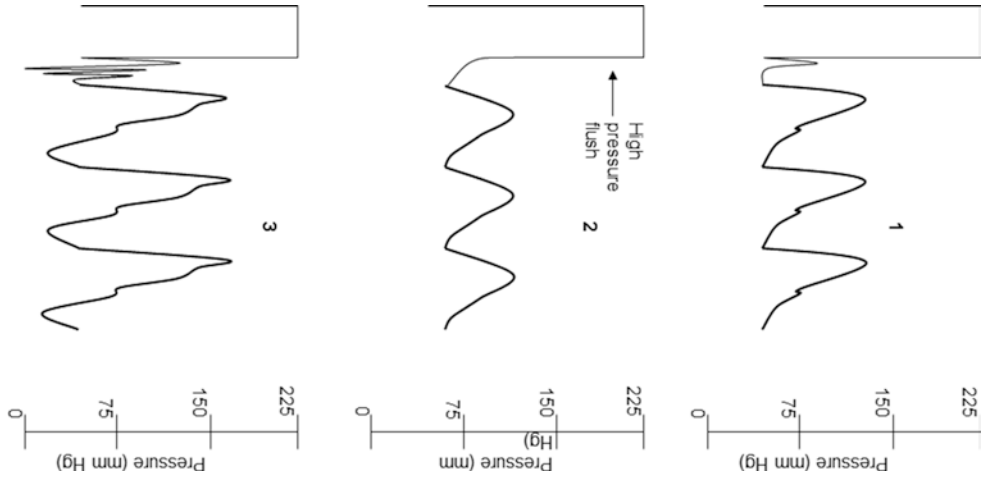

Fig. 20.16 An example of a high-pressure flush test. (*1*) In an optimally damped pressure monitoring system, the pressure wave returns to baseline after one oscillation. (*2*) In an overdamped system, the wave returns to baseline without any oscillations. The systolic blood pressure is underestimated and diastolic pressure overestimated. (*3*) In an underdamped system, the wave oscillates multiple times before returning to baseline. The arterial wave is amplified. The systolic pressure is overestimated and diastolic pressure underestimated. The mean arterial pressure usually is not significantly affected by overdamping or underdamping

Table 20.2 Relative intracardiac pressures in the healthy heart

Pressures	Mean	Range
Left atrium	8	4–12
Left ventricle systolic	125	90–140
Left ventricle end diastolic	8	4–12
Right atrium	5	2–12
Right ventricle systolic	25	15–30
Right ventricle end diastolic	5	0–10
Pulmonary artery systolic	23	15–30
Pulmonary artery diastolic	10	5–15
Pulmonary capillary wedge	10	5–15
Mean pulmonary artery	15	10–20

Table 20.3 Cardiac hemodynamic parameters (normal ranges)

Hemodynamic parameter	Derived formula	Range
CO	HR × SV	4–6 L/min
CI	CO/BSA	2.6–4.3 L/min/m^2
SV	CO × 1000/HR	50–120 mL/beat
SI	SV/BSA	30–65 mL/beat/m^2
SVR	(MAP − CVP) × 80/CO	800–1400 dyne s cm^{-5}
SVRI	(MAP − CVP) × 80/CI	1500–2300 dyne s cm^{-5} m^2
PVR	(PAP − PCWP) 80/CO	140–250 dyne s cm^{-5}
PVRI	(PAP − PCWP) 80/CI	240–450 dyne s cm^{-5} m^2
LVSWI	1.36 (MAP − PCWP) SI/100	45–60 g m/m^2
RVSWI	1.36 (PAP − CVP) SI/100	5–10 g m/m^2

BSA body surface area, *CI* cardiac index, *CO* cardiac output, *CVP* central venous pressure, *HR* heart rate, *LVSWI* left ventricular stroke work index, *MAP* mean arterial pressure, *PAP* pulmonary artery pressure, *PCWP* pulmonary capillary wedge pressure, *PVR* pulmonary vascular resistance, *PVRI* pulmonary vascular resistance index, *RVSWI* right ventricular stroke work index, *SI* stroke index, *SV* stroke volume, *SVR* systemic vascular resistance, *SVRI* systemic vascular resistance index

atrium and the inferior and superior vena cavae. The central venous pressure (Tables 20.2 and 20.3) is an estimate of right heart filling pressures and may be used to assess right heart function and circulating blood volume. The central venous pressure is dependent upon multiple factors such as intravascular volume, functional capacitance of veins, and status of the right heart. A limitation of central venous pressure monitoring is that it does not give direct information about the left heart function. Indications for central venous catheter placement may include monitoring of cardiac filling pressures, administration of drugs, and/or rapid infusion of large amounts of fluids (Table 20.4). A typical central venous pressure kit is shown in JPG 20.7 (online). It is critical to properly calibrate and position the pressure transducer system at the level of the right atrium. Since the numeric value of central venous pressure is small (2–12 mmHg), minor changes in transducer height will cause significant inaccuracies in central venous pressure assessment.

There are multiple sites for placement of central venous catheters. Common sites used in clinical practice are the internal jugular and subclavian veins (Online JPG 20.8). Central venous access can also be accomplished by placement of a long catheter via the antecubital, external jugular, and femoral veins. Complications of central venous catheter placement may include inadvertent arterial puncture (i.e., carotid and subclavian arteries), venous air embolism, pneumothorax, chylothorax, loss of guide wire, nerve injury,

Table 20.4 Relative indications for using a central venous pressure catheter

Large fluid shifts
Vascular access
Infusion of medication
Venous blood sampling
Major trauma and surgery
Monitoring of intravascular volume status
Aspiration of venous air embolus

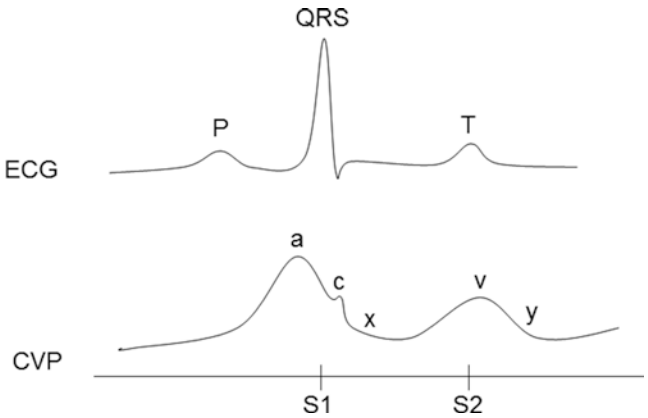

Fig. 20.17 A typical example of a central venous pressure waveform consisting of ***a***, ***c***, and ***v*** waves and ***x*** and ***y*** descents. The ***a*** wave is associated with atrial contraction. The ***c*** wave occurs as the tricuspid valve bulges up toward the right atrium during early ventricular systole. The ***v*** wave is associated with passive filling of the right atrium with closed valve. The ***x*** descent corresponds to the tricuspid valve being pulled down toward the right ventricle during late systole. The ***y*** descent corresponds with opening of the tricuspid valve as the right atrium begins to empty. *CVP* central venous pressure, *ECG* electrocardiogram

cardiac dysrhythmias, and/or line infections. There are multiple types of central venous catheters ranging from a single lumen to multiple lumen (double, triple, quad) catheters. Typically, multilumen catheters have slower flow rates due to the smaller radii of these lumens; recall that resistance to flow is proportional to the fourth power of the radius. After placement of a central venous pressure catheter, all ports must be aspirated and flushed to confirm proper intravascular placement of the catheter and eliminate any potential air in the line. The use of ultrasound for placement of a central venous line is currently common practice and has reduced the incidence of inadvertent arterial punctures. In clinical practice, a chest X-ray is often obtained to confirm proper positioning of the catheter. If a pneumothorax develops after accidental puncture of a lung, it will also be evident on chest X-ray.

The central venous pressure waveform can provide important information about the mechanical events occurring during a cardiac cycle (Fig. 20.17). An ***a*** wave is caused by atrial contraction which occurs after the P-wave on the

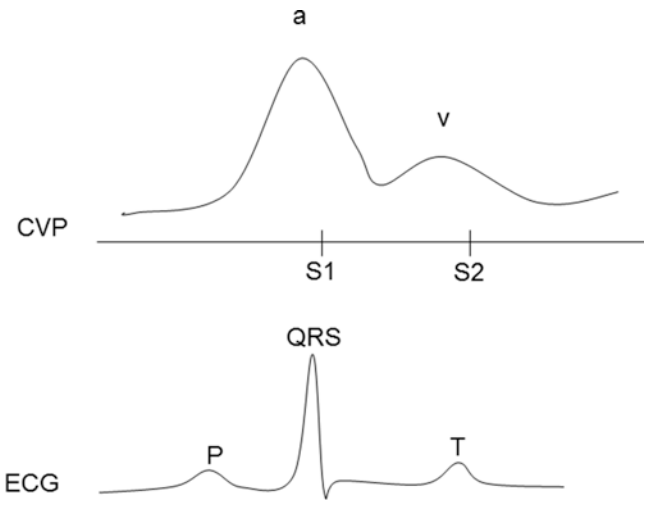

Fig. 20.18 An example of cannon ***a*** waves. A severely stenotic tricuspid valve or a junctional rhythm (atrium contracting against a close tricuspid valve) causes a large *a* wave. The mechanical events of the waveform must be correlated with the electrical events of the ECG

ECG. The ***c*** wave occurs during the start of ventricular systole as the tricuspid valve is pushed up toward the right atrium. The next portion of the waveform is the ***x*** descent, which represents the tricuspid valve being pulled down toward the right ventricle in late systole. The ***v*** wave correlates with passive filling of the right atrium while the tricuspid valve is closed. The ***y*** descent completes the waveform and represents the opening of the tricuspid valve, passive emptying of the right atrium, and filling of the right ventricle during diastole. Again it should be noted that the central venous pressure waveform provides information primarily concerning the right heart. Yet, the same waveform can be observed for the left heart by recording the pulmonary capillary wedge pressure from a pulmonary artery catheter (discussed later in this chapter). The central venous pressure waveform is affected by respirations; thus it should be read at end expiration. There will be central venous pressure variation with each respiratory cycle. Central venous pressure value is typically defined as the mean venous pressure at the end of exhalation during spontaneous or controlled ventilation. At end expiration, the intrathoracic pressure is closest to atmospheric pressure.

There are multiple clinical conditions that will affect the recorded central venous pressure waveform. For example, tricuspid stenosis may result in large (*cannon*) ***a*** waves (Fig. 20.18) as the right atrium contracts and pushes blood past a stenotic valve. Abnormal cardiac nodal rhythms, ventricular arrhythmias, or heart block will result in cannon ***a*** waves, as the atrium and ventricle are not synchronized and the atrium may be contracting against a closed tricuspid valve. Large ***a*** waves may also occur during situations where the resistance to right atrium emptying is significantly

increased, as in tricuspid and pulmonary valve stenosis, right ventricular hypertrophy, and/or pulmonary artery hypertension. Regurgitant valve disorders such as tricuspid regurgitation will result in large ***v*** waves (Fig. 20.19), representing overfilling of the atrium. Specifically, the large ***v*** wave occurs as blood volume from the right ventricle back flows into the right atrium past the incompetent tricuspid valve during systole. A noncompliant right ventricle, as in ischemia and heart failure, may also result in large ***v*** waves. During atrial fibrillation, ***a*** waves are absent due to ineffective atrial contractions. Again, similar waveforms for the left heart are seen from a pulmonary capillary wedge pressure waveform. Diagrams of cannon ***a*** and ***v*** waves are displayed in Figs. 20.18 and 20.19.

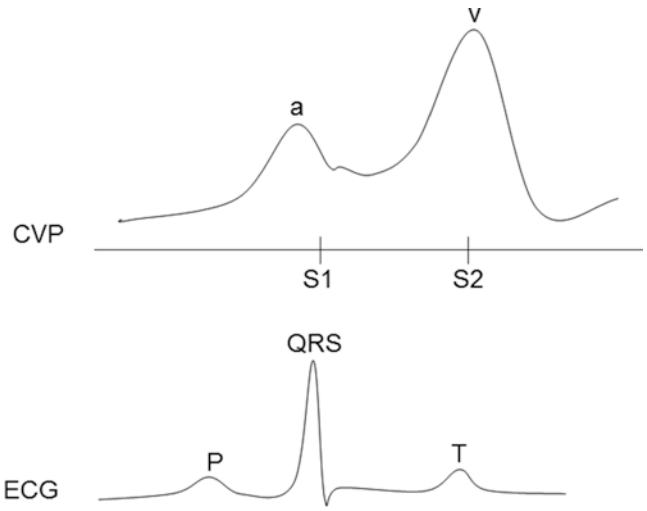

Fig. 20.19 An example of cannon ***v*** waves. An incompetent tricuspid valve (tricuspid regurgitation) abolishes the ***x*** descent and causes cannon ***v*** waves, as volume from the right ventricle back flows into the right atrium during ventricular systole. *CVP* central venous pressure, *ECG* electrocardiogram

20.6 Pulmonary Artery Pressure Monitoring

The pulmonary artery catheter was first introduced into clinical practice by Swan and Ganz [16]. Since its introduction, the pulmonary artery catheter has often been used in the management of critically ill patients and in those undergoing major cardiac surgery (Table 20.5) or solid organ transplantation surgeries. The effectiveness of pulmonary artery catheter monitors and their effect on patient morbidity and mortality continues to be debated and researched [17]. Current modifications also allow for continuous monitoring of pulmonary artery pressure, cardiac output, central venous pressure, mixed venous oxygen saturation (S_VO_2), and pulmonary capillary wedge pressure (Fig. 20.20, Online JPG 20.9).

Table 20.5 Relative indications for using a pulmonary artery catheter

Major organ transplant (liver, heart, lung)
Cardiopulmonary bypass surgery
Pulmonary hypertension
Sepsis/shock
Aortic aneurysm surgery
Heart failure (right and/or left heart)
Pulmonary embolus

See ASA Guidelines for more detailed indications and contraindications [35]

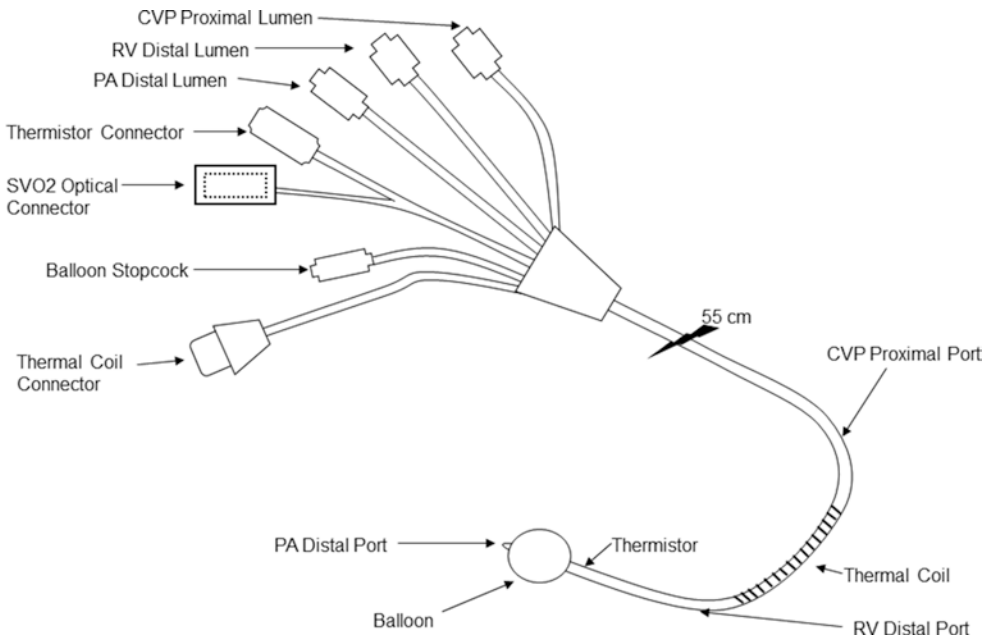

Fig. 20.20 A diagram of a typical pulmonary artery catheter with continuous cardiac output and mean venous oxygen saturation monitoring capabilities. Notice the addition of the thermal coils, thermistors, and optical components to the catheter. Diagram courtesy of Sock Lake Group, LLC. *CVP* central venous pressure, *PA* pulmonary artery, *RV* right ventricle, *SVO2* venous oxygen saturation

One of the advantages of the pulmonary artery catheter is that blood pressure information associated with the left heart may also be obtained via the pulmonary capillary wedge pressure. Under conditions of normal pulmonary physiology and left ventricular function and compliance, the pulmonary capillary wedge pressure is proportional to the left ventricular end-diastolic pressure, which is proportional to left ventricular end-diastolic volume. Left ventricular preload is best measured by left ventricular end-diastolic volume:

$$\text{CVP} \sim \text{PAD} \sim \text{PCWP} \sim \text{LAP} \sim \text{LVEDP} \sim \text{LVEDV}$$

where CVP = central venous pressure, PAD = pulmonary artery diastolic pressure, PCWP = pulmonary capillary wedge pressure, LAP = left atrial pressure, LVEDP = left ventricular end-diastolic pressure, and LVEDV = left ventricular end-diastolic volume.

Typically, after establishing central venous access, a pulmonary artery catheter is floated into the pulmonary artery with the catheter balloon inflated (Online Video 20.1). The location of the pulmonary artery catheter balloon is monitored by analysis of the waveform as the catheter is floated from the vena cava to the right atrium, to the right ventricle, and ultimately into the pulmonary artery (Fig. 20.21). Once the catheter is in the pulmonary artery, it is advanced further until the balloon wedges into a distal arterial branch (smaller diameter) of the pulmonary artery (Fig. 20.22). The resultant mean pressure and waveform is the pulmonary capillary wedge pressure. Under normal physiologic conditions, this pressure correlates well with the left atrial pressure. However, the pulmonary artery catheter balloon should not be kept inflated for a long duration or kept in a wedged position due to the possibility of causing pulmonary artery rupture. Note that whenever the catheter is advanced, the balloon (Online JPG 20.10) should be inflated, and when it is pulled back, the balloon should be deflated. The balloon on most pulmonary artery catheters holds a specific volume of air (1.5 mL). Exceeding this volume may result in balloon rupture and/or catastrophic pulmonary artery rupture. Most currently available catheter systems come with a balloon inflation syringe (built-in limiter) which minimizes the risk of such an error.

As with all pressure transducers, the pulmonary artery catheter pressure transducer must be accurately calibrated and zeroed prior to obtaining pressure readings. The pressure transducer should be zeroed at the level midway between the anterior and posterior chest at the level of the sternum; this is usually near the level of the right atrium. The pulmonary artery pressure should be obtained at end expiration (either during spontaneous or mechanical ventilations).

Proper positioning of the pulmonary artery catheter in the lung region is important in obtaining accurate pressure measurements. Since a greater portion of blood flow goes to the right lung (approximately 55 %), the balloon of the pulmonary artery catheter most often floats to the right pulmonary artery. West et al. categorized three lung zones (I, II, III) based on the correlation between pulmonary arterial pressure, alveolar pressure, and venous pressure [18]. Ideal placement of the pulmonary artery catheter requires the catheter tip to be in zone III. This is the area in the lung where blood flow is uninterrupted and therefore capable of transmitting the most accurate blood pressure; it is also the zone least affected by airway pressures. In order for the pulmonary capillary wedge pressure to best correlate with left atrial pressure, the distal tip of the catheter should be in a patent vascular bed. If the catheter tip is in the area of the lung where alveolar pressure is greater than perfusion pressure, the pulmonary capillary wedge pressure will reflect the alveolar pressure and not left atrial pressure. Controlled mechanical ventilation utilizing positive end-expiratory pressure decreases the size of west zone III and may affect correlation of pulmonary capillary wedge pressure and left atrial pressure [13]. Other clinical settings in which pulmonary capillary wedge pressure may not accurately reflect left atrial pressure include patients with pulmonary vascular disease, mitral valve disease, and chronic obstructive pulmonary disease and/or those being administered with positive end-expiratory pressure [19]. It is possible to convert zone III into

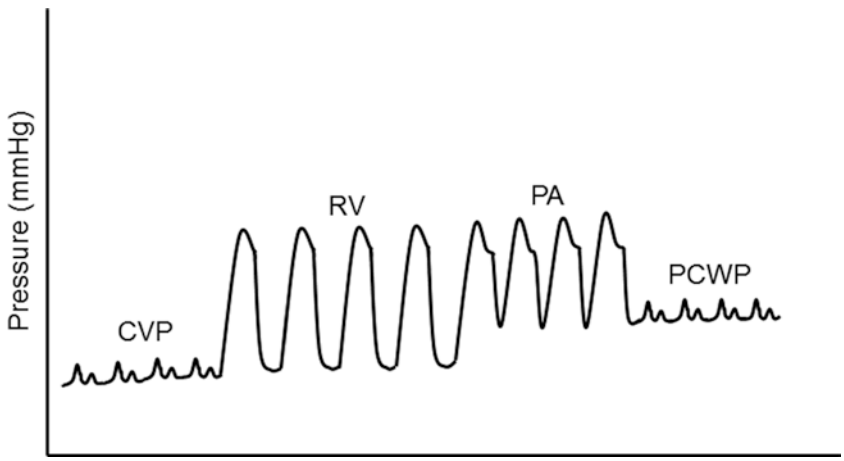

Fig. 20.21 A typical example of right heart blood pressure waveforms. As the pulmonary artery catheter is floated into the distal pulmonary artery, the morphology of the pressure wave changes as it goes through the chambers of the heart. *CVP* central venous pressure, *PA* pulmonary artery pressure, *PCWP* pulmonary capillary wedge pressure, *RV* right ventricle pressure

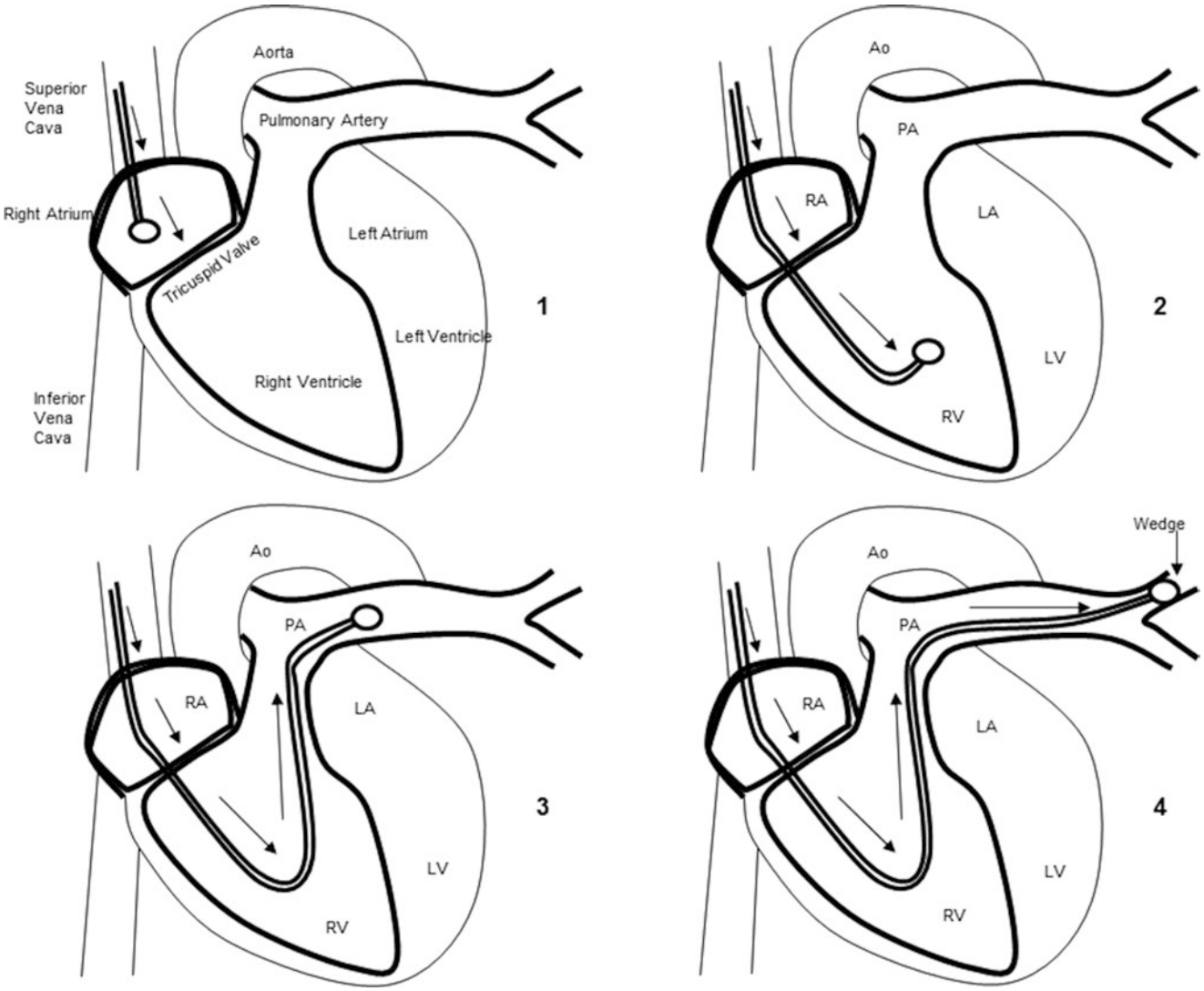

Fig. 20.22 Floating a pulmonary artery catheter through chambers of a heart until the balloon wedges in the distal pulmonary artery. Diagram courtesy of Sock Lake Group, LLC. *Ao* aorta, *LA* left atrium, *LV* left ventricle, *PA* pulmonary artery, *RA* right atrium, *RV* right ventricle

zone II and even zone I, with major increases in pulmonary alveolar pressure, such as positive pressure ventilation and positive end-expiratory pressure [20]. Again, conditions such as positive pressure ventilation, obstructive and restrictive lung disease, and cardiac diseases (i.e., valvular and altered ventricular compliance, tachycardia, and pneumonectomy) are situations where pulmonary capillary wedge pressure does not accurately correlate with left ventricular end-diastolic pressure [21, 22] and hence left ventricular end-diastolic volume.

The pulmonary capillary wedge pressure waveform is similar to the central venous pressure waveform and occurs at a similar time point within the cardiac cycle. Myocardial changes (i.e., myocardial ischemia), which commonly occur in compliance, and valvular disease will affect the waveform. Large ***v*** waves occur with mitral regurgitation, myocardial ischemia, papillary muscle dysfunction, and infarction (Fig. 20.19). Large ***v*** waves may look similar to the pulmonary artery waveform. To prevent errors in interpreting pulmonary capillary wedge pressure and pulmonary artery pressure, the waveform must be viewed and correlated with the ECG tracing. The ***v*** wave will always occur after the QRS complex and peak systemic arterial waveform and will not have a dicrotic notch. The pulmonary artery waveform has a dicrotic notch. A large ***a*** wave typically occurs in patients with mitral stenosis and/or left ventricular hypertrophy.

Pulmonary artery catheters may be contraindicated in patients with known abnormal anatomy of the right heart, such as tricuspid and pulmonic valve stenosis or masses in the right heart. Such catheters may also be contraindicated in patients with left bundle branch block of the myocardial con-

duction system; floating the pulmonary artery catheter through the right heart may cause right bundle branch block and increase the risk of developing complete heart block. The existence of cardiac pacer leads is not a contraindication but may make placement of a pulmonary artery catheter difficult (Online Video 20.2). Care also must be taken when removing such a catheter. Reported complications associated with pulmonary artery catheters include: cardiac arrhythmias, heart block, pulmonary artery rupture, infection, and/or pulmonary infarction [23]. During cardiac surgery such as lung and heart transplant, it is possible to have the pulmonary artery catheter inadvertently sutured in the surgical field. Note that any resistance to catheter removal must alert the clinician to the above possibility.

20.7 Cardiac Output/Cardiac Index Monitoring

Determining cardiac output is now considered vital when managing any critically ill patient, in particular those with severe cardiac disease, pulmonary disease, and/or multiorgan failure. Cardiac output is the total blood flow by the heart measured in liters per minute (L/min); in an average adult, cardiac output is approximately 5–6 L/min. Cardiac output is often equated with global ventricular systolic function. Any increase in demand for oxygen delivery is usually accomplished with an increase in cardiac output. Furthermore, increasing cardiac output is an important factor in oxygen delivery. Cardiac output is dependent upon heart rate and stroke volume. In a normal heart, stroke volume is dependent upon preload, afterload, and contractility. Note that myocardial wall motion abnormalities and/or valvular dysfunction will also affect stroke volume.

Starling's law describes the relationship between cardiac output and left ventricular end-diastolic volume (Fig. 20.3). As preload is increased, the cardiac output increases in direct proportion to the left ventricular end-diastolic volume until an excessive preload is reached. At this point, increases in left ventricular end-diastolic volume do not result in increased cardiac output and may actually decrease it.

Due to variations in body size and weight, cardiac output is frequently expressed as a cardiac index. Cardiac index is equal to cardiac output divided by body surface area and has a normal range of 2.5–4.3 L/min/m^2:

$$\mathrm{CO} = \mathrm{HR} \times \mathrm{SV}$$

$$\mathrm{CI} = \mathrm{CO} / \mathrm{BSA}$$

where CO = cardiac output, HR = heart rate, SV = stroke volume, CI = cardiac index, and BSA = body surface area.

The equation for cardiac output can also be derived by rearranging the oxygen extraction equation. Oxygen extraction is the product of cardiac output and the difference between arteriovenous oxygen content:

$$\mathrm{VO}_2 = \mathrm{CO} \times \left(\mathrm{CaO}_2 - \mathrm{CvO}_2\right)$$

where VO_2 = oxygen extraction, CO = cardiac output, CaO_2 = arterial oxygen content, and CvO_2 = venous oxygen content.

Rearranging the oxygen extraction equation allows calculation of cardiac output:

$$\mathrm{CO} = \mathrm{VO}_2 / \left(\mathrm{CaO}_2 - \mathrm{CvO}_2\right)$$

A limitation of the Fick method is that frequent blood samples from the arterial and venous circulation are required. Expiratory gas must also be analyzed to measure oxygen consumption.

Cardiac output can also be measured by utilizing an indicator (dye) dilution technique or a thermodilution technique. In the indicator dilution technique, a nontoxic dye (e.g., methylene blue or indocyanine green) is injected into the right heart. The dye mixes with blood and goes out the pulmonary artery to the systemic circulation. A circulating arterial blood sample with diluted indicator dye is collected and measured using spectrophotometric analysis. Repeat cardiac output measurements utilizing the indicator dilution technique are limited due to increasing concentrations of dye with each subsequent measurement.

The thermodilution method to measure cardiac output is a modification of the indicator dilution technique initially described by Fegler [24] in 1954. Thermodilution techniques are not considered to be affected by recirculation, as are the indicator dilution techniques. Typically, the distal tips of the pulmonary artery catheters contain thermistors that detect temperatures of circulating blood. The more proximal portion of the pulmonary artery catheter contains an opening that allows for injection of fluid such as normal saline or D_5W. The injected solution may be at an ambient temperature or iced. An iced solution increases the temperature difference and therefore the signal-to-noise ratio [25]; thus, it is considered better than an injectate at room temperature. A computer program within the monitoring system commonly calculates the cardiac output utilizing the thermodilution cardiac output equation. Components of the equation include the following: specific heat of blood, specific gravity of blood and injectate, volume of injectate, and area of blood temperature curve. A modified Stewart-Hamilton equation [26] can also be used to calculate cardiac output using this approach:

$$\mathrm{CO} = \mathrm{V}\left(\mathrm{Tb} - \mathrm{Ti}\right) \times K1 \times K2 / \int \mathrm{Tb}(t)\,dt$$

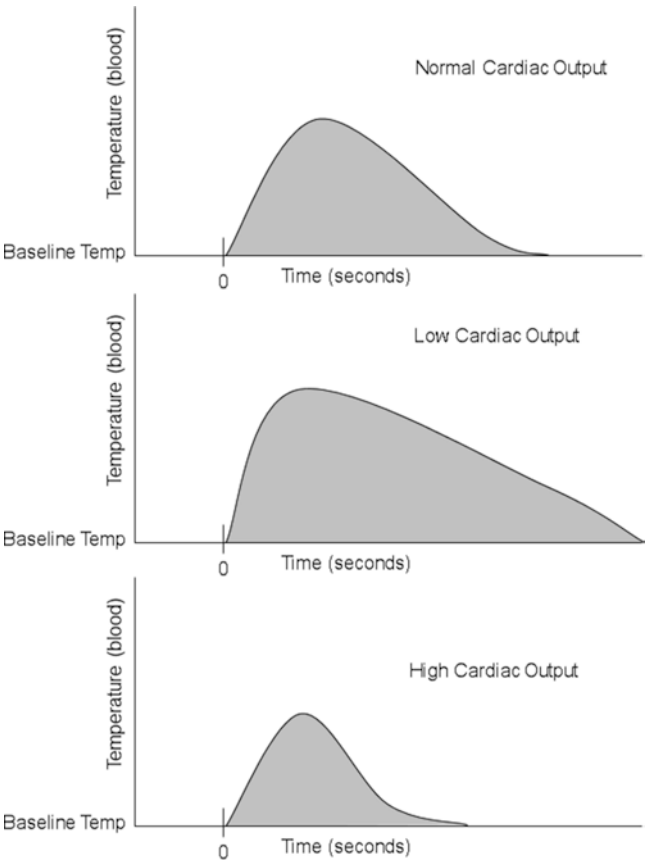

Fig. 20.23 An example of cardiac output monitoring. In this case, cardiac output is inversely proportional to the area under the thermodilution curve

where CO = cardiac output in L/min, V = volume of injectate (mL), Tb = initial blood temperature (°C), Ti = initial injectate temperature, $K1$ = density factor, $K2$ = computation constant, and $\int \Delta \mathrm{Tb}(t)dt$ = integral of blood temperature change over time.

Cardiac output is inversely proportional to the area under the curve (Fig. 20.23).

Nevertheless, an accurate calculation of cardiac output requires both proper position of the pulmonary artery catheter and a consistent volume of injectate. Note that conditions such as tricuspid and pulmonic value regurgitation and intracardiac shunts will cause recirculation of blood and thus result in the false elevation of cardiac output. The errors of intermittent bolus thermodilution techniques include valuable volumes and temperatures of injectate, technique of injection, and timing of injection with the respiratory cycle [27]. Cardiac output measurements are also affected by clinical conditions such as tricuspid insufficiency, intracardiac shunts, and/or atrial fibrillation [19].

More recently, continuous cardiac output monitoring has been made possible with advanced pulmonary artery catheters (Online JPG 20.11). Typically, continuous cardiac output monitors utilize a thermal coil which is positioned in the right ventricle; this coil intermittently heats the blood. Once the continuous cardiac output catheter and system reaches a steady state with its surroundings, the thermal coil intermittently heats blood. The temperature change of the surrounding blood is detected by a thermistor located at the distal tip of the pulmonary artery catheter; the recorded blood temperature varies inversely with cardiac output.

The accuracy of the system depends on the measurement of temperature differences from the injection port to the distal measurement thermistor. In the thermodilution technique, the volume of injectate must be constant (10 mL). Smaller amounts of cold solution reaching the thermistor will result in a higher cardiac output. Such detected differences may be caused by actual increased cardiac output, small amounts of injectate, warm indicator and/or injectate, a clot on the thermistor, or a wedged catheter. A calculated small cardiac output will result when the solution reaching the thermistor is too cold; this may occur if there is too large an amount of injectate, if the solution is too cold, if there is an actual decrease in cardiac output, and/or if the patient has an intracardiac shunt. A major limitation of continuous cardiac output method is its slow response time to acute changes in cardiac output [27, 28]. Although the response time may be slow, it is still faster in detecting cardiac output changes than the traditional intermittent thermodilution technique. Furthermore, continuous cardiac output monitoring is generally considered to be more accurate than the intermittent thermodilution technique [29, 30].

Noninvasive methods to measure cardiac output include Doppler modalities, the transpulmonary dilution technique [31, 32], gas rebreathing technology [32, 33], and/or a bioimpedance [32, 34, 35] technique. Briefly, the noninvasive Doppler method to measure cardiac output is an esophageal Doppler monitor. As such, an esophageal Doppler probe is placed and an ultrasound beam is directed at the descending aorta. By knowing the cross-sectional area of the aorta and blood velocity, the stroke volume is calculated [32].

The transpulmonary dilution method for measuring cardiac output requires injections of an indicator (lithium or thermodilution) in the venous circulation (central or peripheral) and subsequent assessment of the indicator level of the systemic arterial circulation; a typical example is the lithium chloride solution technique [36–38]. Lithium chloride indicator is injected through a central or peripheral vein, and the plasma concentration of this indicator is measured via a lithium-specific electrode connected to the arterial line [39]. A concentration-time curve is generated and cardiac output is calculated from the area under the curve associated with the lithium ion concentrations [40].

The thoracic bioimpedance method measures cardiac output by detecting the change in flow of electricity with alteration in blood flow [31]. For thoracic bioimpedance, a low-amplitude and high-frequency current is transmitted and

then sensed by sets of electrodes placed on both sides of the thorax and neck. The cardiac alterations in impedance (resistance to current flow) are analyzed and calculated as the blood volume changes for each heart beat (stroke volume). The thoracic bioimpedance method of measuring cardiac output may be useful in clinical situations such as major trauma [41, 42] and cardiac disease [43].

Gas technology utilizing the measurement of carbon dioxide [32, 44] applies the Fick principle of oxygen consumption and cardiac output but substitutes carbon dioxide production for oxygen consumption. By determining the change in CO_2 production and end-tidal CO_2, modification of the Fick equation can be applied to calculate cardiac output [45]:

$$CO = \quad VCO_2 / \quad EtCO_2$$

where CO = cardiac output, ΔVCO_2 = change in CO_2 production, and $\Delta EtCO_2$ = end-tidal CO_2.

It should be noted that the accuracy of the carbon dioxide rebreathing method to measure cardiac output is, at present time, inconclusive [45–48].

20.8 Mixed Venous Saturation Monitoring (SvO_2)

Mixed venous oxygen saturation monitoring (SvO_2) typically utilizes reflective spectrophotometric technology to measure the amount of oxygen in mixed venous blood. Yet, a true mixed venous blood sample is measured in the pulmonary artery. Systemic venous blood with different oxygen extraction ratios returns to the right atrium via the superior vena cava and inferior vena cava, mixes and equilibrates in the right ventricle, and flows out past the pulmonic valve to the pulmonary artery. As blood travels past the SvO_2, catheter light emitted from the catheter tip is reflected off the red blood cells and is detected by a photodetector. The difference in wavelengths of emitted and reflected light is processed to estimate SvO_2 (Fig. 20.24). Continuous venous saturation (SvO_2) monitoring has been made possible with the adaptation of a pulmonary artery catheter with fiber-optic technology (Online JPG 20.11). Such monitoring utilizes the principle of reflectance spectrophotometry, which uses multiple wavelengths of transmitted light at specific intensities that is then reflected from red blood cells. For example, oxygenated hemoglobin absorbs most infrared light (940 nm) and reflects or transmits most red light (660 nm); this is the reason that oxyhemoglobin looks red and deoxyhemoglobin appears blue. The tip of the SvO_2 catheter emits light with specific wavelengths which measure both oxyhemoglobin and deoxyhemoglobin, as red blood cells flow past the tip of the catheter. The difference between absorption of light between saturated and desaturated hemoglobin results in the calculated SvO_2 value.

The SvO_2 equation is a modification of the Fick equation; SvO_2 is derived by rearranging the Fick equation as follows:

$$VO_2 = C(a-v)O_2 \times CO \times 10$$

$$SvO_2 = SaO_2 - VO_2 / DO_2$$

$$DO_2 = \text{volume of } O_2 \text{ delivered per minute} = CO \times CaO_2 \times 10$$

$$VO_2 = \text{oxygen consumption per minute} = C(a-v)O_2 \times CO \times 10$$

$$SaO_2 = \text{arterial } O_2 \text{ saturation}(1.0)$$

$$CaO_2 = 1.39 \times Hgb \times SpO_2 + 0.003 \times PaO_2$$

where VO_2 = oxygen consumption, CaO_2 = arterial oxygen content, CvO_2 = venous oxygen content, CO = cardiac output, DO_2 = oxygen delivery, SaO_2 = arterial oxygen saturation, Hgb = hemoglobin, SpO_2 = oxygen saturation, and PaO_2 = partial pressure of arterial oxygen.

Accurate measurement of SvO_2 requires that vasoregulation be intact [49], and there must be a continuous flow of

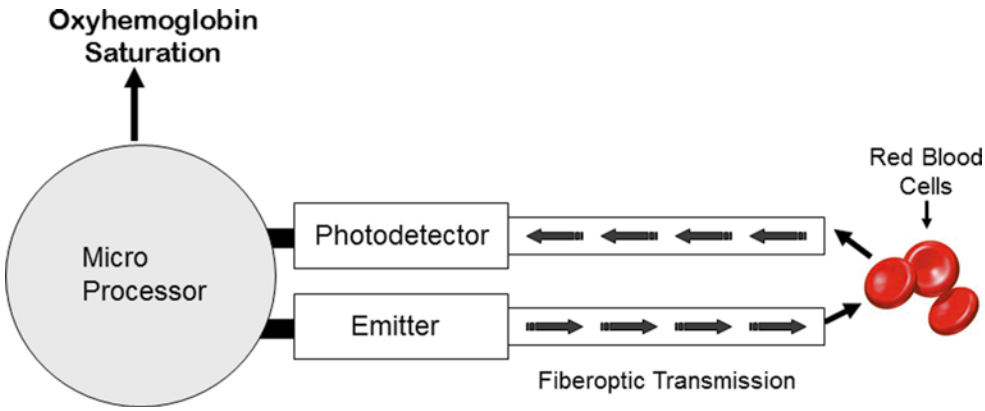

Fig. 20.24 An example of mixed venous saturation monitoring (*SvO2*). Spectrophotometric technology such as pulse oximeter and mixed venous oxygen saturation monitors are utilized to measure the amount of oxygenated hemoglobin in circulating blood. A specific wavelength (infrared) is emitted and the reflected wavelength off the red blood cells is detected and processed

blood past the tip of the catheter. SvO_2 values may be incorrect if the tip of the pulmonary artery catheter migrates into the distal pulmonary artery and/or comes in contact with the arterial wall. Other causes of incorrect SvO_2 values include miscalibration of the microprocessor or light intensity that is too low (some sensor systems have incorporated intensity monitors). Note that the tip of the catheter must be in the pulmonary artery in order to have true mixed venous oxygen.

Mixed venous oxygen saturation (SvO_2) monitoring provides information about the balance between total body oxygen consumption and delivery. SvO_2 (0.65–0.75) measures the amount of oxygen not taken up by organs and tissues. Therefore, the lower the SvO_2, the higher the fraction extraction of oxygen by the tissues and a possible imbalance between oxygen consumption and oxygen delivery. SvO_2 is dependent upon arterial oxygen saturation, oxygen consumption, concentration of hemoglobin, and cardiac output. A significant change in SvO_2 may be caused by decreased oxygen delivery (decreased cardiac output and hemoglobin), increased oxygen consumption, or decreased arterial oxygen saturation. Continuous SvO_2 monitoring is useful in conditions where there is significant oxygen transport imbalance including: severe cardiac and respiratory disease, sepsis, and/or dysfunctional oxygen transport [50]. During stable arterial oxygen content and consumption, SvO_2 reflects the relative cardiac output [51, 52]. Furthermore, monitoring of SvO_2 may provide vital information in the medical management of critically ill [53, 54] and/or cardiac surgery patients [55]. If SvO_2 drops during a period of increased oxygen demand, it may indicate inadequate tissue perfusion and oxygen delivery; this information would not be available with monitoring cardiac output only.

It is considered that SvO_2 may be a better measurement of myocardial performance than cardiac output alone. Acute decrease in SvO_2 below 0.65 indicates a disparity between oxygen delivery and oxygen consumption. A change in SvO_2 greater than ±0.1 is considered significant. Medical management of critically ill patients by implementing measures to keep SvO_2 normal is considered important for decreasing morbidity and mortality [39, 56]. Conditions where SvO_2 is greater than 0.75 include increased oxygen delivery and low oxygen consumption. SvO_2 may be elevated during septic shock, hyperoxygenation, and cyanide toxicity and in patients with arterial venous shunts [49, 50]. The increase in SvO_2 during sepsis is considered, in part, due to the loss of vasoregulation and yet does not mean that organ tissues are being adequately oxygenated. It should be noted that, under general anesthesia, the SvO_2 value is increased due to the decreased metabolic requirement for oxygen by tissues.

In clinical settings where a pulmonary artery SvO_2 catheter is not possible (i.e., pediatric patients), a central venous oxygen saturation ($ScvO_2$) monitor may be used. The advantage of $ScvO_2$ is that a pulmonary artery catheter is not required; only central venous access is needed. The $ScvO_2$ obtains venous oxygen saturation readings from the superior vena cava or right atrium. During normal physiological and hemodynamic conditions, $ScvO_2$ correlates well with SvO_2 [57–59]. However, in critical illness and shock, the $ScvO_2$ does not accurately reflect the true SvO_2 [60–62] and, therefore, true SvO_2 can only be measured in the pulmonary artery in such cases [63]. Resuscitation and medical management of critically ill patients with a $ScvO_2$ monitor may provide benefits over conventional monitors such as vital signs and/or central venous pressure [60].

20.9 Flow Monitoring

While cardiac output is similar regardless of where it is measured within the heart, the flow profiles can change dramatically within different anatomical structures and disease states. Given a constant cardiac output, flow velocity increases with a smaller diameter vessel, with larger velocities seen at the center of the flow profile and with zero velocity at the vessel wall.

For example, flow through the cardiac valves is important for diagnoses of stenosis and regurgitation. Stenosis is defined as a narrowing of the orifice area of the valve. This can be caused by a variety of factors including sclerosis formation on leaflets and is characterized by abnormally high flow velocities through the valve. Regurgitation is defined as flow reversal through a valve and can be caused by annular dilatation, leaflet prolapse, and/or changes in chamber dimensions affecting the valve performance. While a small amount of regurgitation is normal (caused by valve closing called the *closing volume*), patients with pathologic regurgitation have abnormally high flows traveling retrograde across the valve orifice.

Clinical diagnoses of regurgitation and stenosis are typically done using echocardiography (see Chap. 22). Pulsed wave Doppler measures a frequency shift in the ultrasound waves to calculate a flow velocity. Color flow mapping allows for visualization of the flow through the valve. By standards, areas flowing toward the transducer head appear red, areas flowing away from the transducer head appear blue, and areas of regurgitation or turbulent flow appear in a third color, typically yellow or green. Flow rates, pressure gradients, and orifice area measurements are available in Table 20.6 for the varying degrees of stenosis for each of the cardiac valves, as reported by the American College of Cardiology (ACC)/American Heart Association (AHA) guidelines [64]. Consult the ACC/AHA guidelines for diagnosing the severity of regurgitation.

In a research setting, several other methods are available for flow monitoring across the cardiac valves in an in vivo setting. Doppler sensors, using the same principles as echocardiography, are available in a number of forms, a c-ring transducer (transonic) being common. This flow probe takes frequency

Table 20.6 Indications for diagnosing stenosis of the cardiac valves

	Jet velocity (m/s)	Pressure gradient (mm Hg)	Orifice area (cm^2)
Aortic stenosis			
Mild	<3.0	<25.0	>1.5
Moderate	3.0–4.0	25.0–40.0	1.0–1.5
Severe	>4.0	>40.0	<1.0
Mitral stenosis			
Mild	<5.0	<30.0	>1.5
Moderate	5.0–10.0	30.0–50.0	1.0–1.5
Severe	>10.0	>50.0	<1.0
Tricuspid stenosis			
Severe	NA	NA	<1.0
Pulmonic stenosis			
Severe	>4.0	>60.0	NA

measurements, calculates a velocity from the measurement, and then multiplies the velocity by the area of the c-ring to determine the flow through the vessel. This type of sensor is useful for flows downstream of the aortic or pulmonary valves but cannot be attached in the atrioventricular positions.

Electromagnetic sensors take advantage of Faraday's law of inductance to measure velocity of a conducting fluid, such as blood. A rapidly reversing magnetic field is produced and, as the fluid moves through this field, a voltage is generated. This voltage is measured and translated into a frequency signal which is proportional to flow rate. Sensors are capable of measuring the instantaneous velocity of a small area with high temporal resolution and can be attached to a catheter. The disadvantage of electromagnetic sensors is that the measurements are affected by catheter placement, the exact location of which can be difficult to determine through fluoroscopy.

Cardiac magnetic resonance can be utilized in both a clinical and research role to investigate flow through valves and major vessels. Phase-contrast cardiac magnetic resonance enables the measurement of blood flow velocity across the cardiac valves and the great vessels with a high temporal and spatial resolution. As blood flows through the static magnetic field, the precession frequency changes in the hydrogen atoms of the tissue. This frequency change results in a dephasing effect on the magnetization of the atoms. The net dephasing of the atomic spins is a function of the velocity of the blood flow as well as the direction. This technique is used for clinical diagnoses of valvular regurgitation and aortic stenosis and to investigate coronary flow. For more information on these methods, the reader is referred to Chap. 24.

Angiograms are utilized to observe acute flow through the coronary system. While this is a qualitative technique for flow monitoring, it is of clinical importance, particularly for the assessment of coronary blockages. In an angiogram, the patient is typically cannulated via a femoral artery and the catheter is fed into or near the coronary ostia. Contrast is then injected through the catheter and into the bloodstream. By imaging via fluoroscopy (continuous X-rays), the contrast can be observed traveling through the coronary system. Flow is considered interrupted anywhere that contrast cannot traverse, indicating a blockage or reduced flow in the coronary system. An arterial dissection of the left anterior descending coronary artery is shown in Online JPG 20.12. The dissection is a tear in the tunica intima of the blood vessel, which allows blood into the space between the inner and outer layers of the vessel wall, resulting in vessel stenosis and possible occlusion. The area of the dissection is circled on the left of the image and the reduction in flow is visible downstream of the dissection. The image on the right shows the same artery after the vessel has healed.

Classification of blood flow using engineering terms is not a simple task. Blood flow through vessels is typically laminar, but partial occlusions can lead to turbulence downstream of the occlusion. This phenomenon is utilized in blood pressure measurements (i.e., Korotkoff sounds). Flow through or near a cardiac valve becomes quite a bit more complicated, as it is neither laminar nor turbulent. Yoganathan et al. classify the pulsatile flow of blood through cardiac valves as *borderline turbulent flow*, characterized by regions of flow reversal, 3D separation, and vortex formation, with borderline turbulent flow being defined as unsteady laminar flow with more than one temporal frequency excited. Yet, they further describe the flow to transition into a fully turbulent state during peak systole [65].

20.10 Implantable Monitoring

In both research and clinical settings, the ability to more optimally and continuously monitor hemodynamic properties is being realized. Furthermore, devices are being developed for researchers who work with small animals, for clinical researchers, and for physicians to monitor their patients without clinical visits. These devices may consist of sensors that transmit data to an implantable loop recorder, where the information is stored until it is collected by the researcher or physician by telemetry or other means.

An implantable loop recorder is a valuable tool for researchers conducting chronic studies and for clinicians. For example, data can be collected continuously when investigating properties that occur only rarely or change slowly over time. Clinically, implantable loop recorders that gather ECG data are used for diagnosis of patients with unexplained syncope, near syncope, episodic or recurrent palpitations, and seizure-like events. The use of an implantable loop recorder has diagnosed patients in which standard tilt-table testing has failed to induce syncope [66–68] and is now advised for management of patients with syncope [69, 70]. Two examples of implantable loop recorders are the Sleuth (Transoma Medical, Inc., Arden Hills, MN, USA) and the Reveal Plus (Medtronic, Inc., Minneapolis, MN, USA).

Perhaps the most advanced implantable hemodynamic monitoring system to date is the investigational device called Chronicle (Medtronic, Inc.). It is a pressure sensor-equipped lead that is implanted in the right ventricle to provide continuous hemodynamic monitoring of heart rate, right ventricular systolic pressure, right ventricular diastolic pressure, right ventricular pulse pressure, maximum right ventricular dP/dt, and/or estimated pulmonary artery diastolic pressure [71, 72]. The data storage period of this device can be adjusted with the desired sampling rate but can also be reprogrammed as desired.

Another application of implantable sensors is the monitoring of patients with congestive heart failure. Signs and symptoms of congestive heart failure are not well correlated with the disease status [73, 74]. Investigational devices combining pacing capabilities with monitoring capabilities have been implanted in ambulatory patients with congestive heart failure to monitor parameters such as the mixed venous oxygen saturation and right ventricular pressures. The feasibility of these devices has been shown [75], but clinical validation studies are ongoing.

Implantable monitors are only as valuable as the information they collect and the manner and ease in which that information is transferred to those interpreting it. Collection of the data is less of an issue in a research setting, where the researcher can personally ensure the data is retrieved at the proper time and in the desired format. Clinicians, on the other hand, could have a large number of patients with implantable monitors who reside in a large geographic area. In addition, numerous home telemonitoring units are in use to gather data from patients with implantable devices and send the data to a location where it can be processed and interpreted by their physicians. Examples of telemonitoring systems include the LATITUDE® Patient Management system (Boston Scientific, Inc., Natick, MA, USA) and the CareLink® network (Medtronic, Inc.). The field of implantable cardiac monitoring is growing rapidly and with the advent of printed flexible electronics it will continue to accelerate.

20.11 Summary

Advanced methods and technology continue to develop for the assessment of cardiac hemodynamics. Such monitoring can be used acutely; however, many new technologies are being developed for chronic monitoring of the cardiac patient (e.g., employing miniaturized implantable sensors and noninvasive hemodynamic monitors). In this chapter, we provided a general overview of several devices and/or systems that can be used either clinically or experimentally to monitor cardiac performance. However, it should be reiterated that to best understand how the output of such devices can be used for the assessment of cardiac function, one needs to first possess an in-depth understanding of underlying basic cardiac physiology.

References

1. Sengupta PP, Khandheria BK, Korinek J et al (2006) Apex-to-base dispersion in regional timing of left ventricular shortening and lengthening. J Am Coll Cardiol 47:163–172
2. Ratcliffe MB, Gupta KB, Streicher JT et al (1995) Use of sonomicrometry and multidimensional scaling to determine the three-dimensional coordinates of multiple cardiac locations: feasibility and initial implementation. IEEE Trans Biomed Eng 42:587–597
3. Gorman JH III, Gupta KB, Streicher JT et al (1996) Dynamic three-dimensional imaging of the mitral valve and left ventricle by rapid sonomicrometry array localization. J Thorac Cardiovasc Surg 112:712–725
4. Meyer SA, Wolf PD (1997) Application of sonomicrometry and multidimensional scaling to cardiac catheter tracking. IEEE Trans Biomed Eng 44:1061–1067
5. Geddes LA, Baker LE (1967) The specific resistance of biological material–a compendium of data for the biomedical engineer and physiologist. Med Biol Eng 5:271–293
6. Baan J, van der Velde ET, de Bruin HG et al (1984) Continuous measurement of left ventricular volume in animals and humans by conductance catheter. Circulation 70:812–823
7. van der Velde ET, van Dijk AD, Steendijk P et al (1992) Left ventricular segmental volume by conductance catheter and cine-CT. Eur Heart J 13 Suppl E:15–21
8. White PA, Redington AN (2000) Right ventricular volume measurement: can conductance do it better? Physiol Meas 21:R23–R41
9. Hettrick DA, Battocletti J, Ackmann J, Linehan J, Warltier DC (1998) In vivo measurement of real-time aortic segmental volume using the conductance catheter. Ann Biomed Eng 26:431–440
10. Gardner RM (1996) Accuracy and reliability of disposable pressure transducers coupled with modern monitors. Crit Care Med 24:879–882
11. Skeehan TM, Thys DM (1995) Monitoring of the cardiac surgical patient. In: Hensley FA, Martin DE (eds) A practical approach to cardiac anesthesia, 2nd edn. Little, Brown and Company, Boston, p 102
12. Gorback MS (1988) Considerations in the interpretation of systemic pressure monitoring. In: Lumb PD, Bryan-Brown CW (eds) Complications in critical care medicine. Year Book, Chicago, p 296
13. Shasby DM, Dauber IM, Pfister S et al (1980) Swan-Ganz catheter location and left atrial pressure determine the accuracy of wedge pressure when positive end expiratory pressure is used. Chest 80:666–670
14. Snyder JV, Carroll GC (1982) Tissue oxygenation: a physiologic approach to a clinical problem. Curr Probl Surg 19:650
15. Stanley TE, Reves JG (1994) Cardiovascular monitoring. In: Miller RD (ed) Anesthesia, 4th edn. Churchill Livingstone, Boston, p 1167
16. Swan HJC, Ganz W, Forrester J, Marcus H, Diamon G, Chonette D (1970) Catheterization of the heart in man with use of a flow-directed balloon-tipped catheter. N Engl J Med 283:447–451
17. Practice Guidelines for Pulmonary Artery Catheterization: An Updated Report by the American Society of Anesthesiologists Task Force on Pulmonary Artery Catheterization. Anesthesiology 2003;99:988–1014
18. West JB, Dollery CT, Naimark A (1964) Distribution of blood flow in isolated lung; relation to vascular and alveolar pressures. J Appl Physiol 19:713–724
19. Wesseling KH (1996) Finger arterial pressure measurement with Finapres. Z Kardiol 3:38–44
20. Brandstetter RD, Grant GR, Estilo M, Rahim R, Sing K, Gitler B (1998) Swan-Ganz catheter: misconceptions, pitfalls, and incomplete user knowledge-an identified trilogy in need of correction. Heart Lung 27:218–222

21. Wittnich C, Trudel J, Zidulka A, Chiu RC (1986) Misleading "pulmonary wedge pressure" after pneumonectomy: its importance in postoperative fluid therapy. Ann Thorac Surg 42:192–196
22. Van Aken H, Vandermeersch E (1988) Reliability of PCWP as an index for left ventricular preload. Br J Anaesth 60:85S–89S
23. Stanley TE, Reves JG (1994) Cardiovascular monitoring. In: Miller RD (ed) Anesthesia, 4th edn. Churchill Livingstone, Boston, pp 1184–1185
24. Fegler G (1954) Measurement of cardiac output in anesthetized animals by thermodilution method. Q J Exp Physiol 39:153
25. Pearl RGB, Rosenthal MH, Mielson L et al (1986) Effect of injectate volume and temperature on thermodilution cardiac output determination. Anesthesiology 64:798
26. Reich DL, Moskowitz DM, Kaplan JA (1999) Hemodynamic monitoring. In: Kaplan JA, Reich DL, Konstaelt SN (eds) Cardiac anesthesia, 4th edn. WB Saunders Co, Philadelphia
27. Burchell SA, Yu M, Takiguchi SA, Ohta RM, Myers SA (1997) Evaluation of a continuous cardiac output and mixed venous oxygen saturation catheter in critically ill surgical patients. Crit Care Med 25:388–391
28. de Figueiredo LFP, Malbouisson LMS, Varicoda EY et al (1999) Thermal filament continuous thermodilution cardiac output delayed response limits its value during acute hemodynamic instability. J Trauma 47:288–293
29. Mihaljevi T, vonSegesser LK, Tonz M et al (1995) Continuous versus bolus thermodilution cardiac output measurements: a comparative study. Crit Care Med 23:944–949
30. Mihm FG, Gettinger A, Hanson CW et al (1998) A multicenter evaluation of a new continuous cardiac output pulmonary artery catheter system. Crit Care Med 26:1346–1350
31. Della RG, Costa MG, Pompei L et al (2002) Continuous and intermittent cardiac output measurement: pulmonary artery catheter versus aortic transpulmonary technique. Br J Anaesth 88:350–356
32. Pamley CL, Pousman RM (2002) Noninvasive cardiac output monitoring. Curr Opin Anaesthesiol 15:675–680
33. Christensen P, Clemensen P, Andersen PK et al (2000) Thermodilution versus inert gas rebreathing for estimation of effective pulmonary blood flow. Crit Care Med 28:51–56
34. Imhoff M, Lehner JH, Lohlein D (2000) Noninvasive whole-body electrical bioimpedance cardiac output and invasive thermodilution cardiac output in high-risk surgical patients. Crit Care Med 28:2812–2818
35. Shoemaker WC, Wo CC, Bishop MH et al (1994) Multicenter trial of a new thoracic electrical bioimpedance device for cardiac output estimation. Crit Care Med 22:1907–1912
36. Linton RA, Band DM, Haire KM (1994) A new method of measuring cardiac output in main using lithium dilution. Br J Anaesth 71:262–266
37. Linton R, Band D, O'Brian T et al (1997) Lithium dilution cardiac output measurement: a comparison with thermodilution. Crit Care Med 25:1767–1768
38. Kurita T, Morita K, Kato S et al (1997) Comparison of the accuracy of the lithium dilution technique with the thermodilution technique for measurement of cardiac output. Br J Anaesth 79:770–775
39. Rivers E, Nguyen B, Havstad S et al (2001) Early goal-directed therapy in the treatment of severe sepsis and septic shock. N Engl J Med 345:1368–1377
40. Band DM, Linton RA, Jonas MM et al (1997) The shape of indicator dilution curves used for cardiac output measurement in man. J Physiol 498:225–229
41. Shoemaker WC (2002) New approaches to trauma management using severity of illness and outcome prediction based on noninvasive hemodynamic monitoring. Surg Clin North Am 82:245–255
42. Shoemaker WC, Wo CC, Chan L et al (2001) Outcome prediction of emergency patients by noninvasive hemodynamic monitoring. Chest 120:528–537
43. Drazner MH, Thompson B, Rosenberg PB et al (2002) Comparisons of impedance cardiography with invasive hemodynamic measurements in patients with heart failure secondary to ischemic or nonischemic cardiomyopathy. Am J Cardiol 89:993–995
44. Binder JC, Parkin WG (2001) Non-invasive cardiac output determination: comparison of a new partial-rebreathing technique with thermodilution. Anaesth Intensive Care 28:427–430
45. Maxwell RA, Gibson JB, Slade JB et al (2001) Noninvasive cardiac output by partial CO_2 rebreathing after severe chest trauma. J Trauma 51:849–853
46. Tachibana K, Imanaka H, Miyano H et al (2002) Effect of ventilatory settings on accuracy of cardiac output measurement using partial CO_2 rebreathing. Anesthesiology 96:96–102
47. Botero M, Lobato EB (2001) Advances in noninvasive cardiac output monitoring: an update. J Cardiothorac Vasc Anesth 15:631–640
48. Kotake Y, Moriyama K, Innami Y et al (2003) Performance of noninvasive partial CO_2 rebreathing cardiac output and continuous thermodilution cardiac output in patients undergoing aortic reconstruction surgery. Anesthesiology 99:283–288
49. Keech J, Reed RL II (2003) Reliability of mixed venous oxygen saturation as an indicator of the oxygen extraction ratio demonstrated by a large patient data set. J Trauma 54:236–241
50. Snyder JV, Carroll GC (1982) Tissue oxygenation: a physiologic approach to a clinical problem. Curr Probl Surg 19:650
51. Jain A, Shroff SG, Jnicki JS et al (1991) Relation between venous oxygen saturation and cardiac index. Nonlinearity and normalization for oxygen uptake and hemoglobin. Chest 99:1403–1409
52. Inomata S, Nishikawa T, Taguchi M (1994) Continuous monitoring of mixed venous oxygen saturation for detecting alterations in cardiac output after discontinuation of cardiopulmonary bypass. Br J Anaesth 72:11–16
53. Rivers E, Nguyen B, Vastad S et al (2001) Early goal-directed therapy in the treatment of severe sepsis and septic shock. N Engl J Med 345:1368–1377
54. Kraft P, Steltzer H, Hiesmayr M et al (1993) Mixed venous oxygen saturation in critically ill septic shock patients: the role of defined events. Chest 103:900–906
55. Waller JL, Kaplan JA, Bauman LI et al (1982) Clinical evaluation of a new fiberoptic catheter oximeter during cardiac surgery. Anesth Analg 61:676–679
56. Vedrinne C, Bastien O, De Varax R et al (1997) Predictive factors for usefulness of fiberoptic pulmonary artery catheter for continuous oxygen saturation in mixed venous blood monitoring in cardiac surgery. Anesth Analg 85:2–10
57. Goldman RH, Klughaupt M, Metcalf T et al (1968) Measured central venous oxygen saturation in patients with myocardial infarction. Circulation 38:941–946
58. Berridye JC (1992) Influence of cardiac output on correlation between mixed venous and central venous oxygen saturation. Br J Anaesth 89:409–410
59. Davies GG, Mendehall J, Symrey T (1988) Measurement of right atrial oxygen saturation by fiberoptic oximetry accurately reflects mixed venous oxygen saturation in swine. J Clin Monit 4:99–102
60. Rivers EP, Ander DS, Powell D (2001) Central venous oxygen saturation monitoring in the critically ill patient. Curr Opin Crit Care 7:204–211
61. Lee J, Wright F, Barber R et al (1972) Central venous oxygen saturation in shock: a study in man. Anesthesiology 36:472–478
62. Scheinman MM, Brown MA, Rapaport E (1969) Critical assessment of use of central venous oxygen saturation as a mirror of mixed venous oxygen in severely ill cardiac patients. Circulation 40:165–172
63. Edwards JD, Mayall RM (1998) Importance of the sampling site for measurement of mixed venous oxygen saturation in shock. Crit Care Med 26:1356–1360

64. Bonow RO, Carabello B, de Leon AC et al (1998) ACC/AHA guidelines for the management of patients with valvular heart disease. J Heart Valve Dis 7:672–707
65. Yoganathan AP, Chandran KB, Sotiropoulos F (2005) Flow in prosthetic heart valves: state-of-the-art and future directions. Ann Biomed Eng 33:1689–1694
66. Brignole M, Sutton R, Menozzi C et al (2006) Lack of correlation between the responses to tilt testing and adenosine triphosphate test and the mechanism of spontaneous neurally mediated syncope. Eur Heart J 27:2232–2239
67. Deharo JC, Jego C, Lanteaume A, Djiane P (2006) An implantable loop recorder study of highly symptomatic vasovagal patients: the heart rhythm observed during a spontaneous syncope is identical to the recurrent syncope but not correlated with the head-up tilt test or adenosine triphosphate test. J Am Coll Cardiol 47:587–593
68. Moya A, Brignole M, Menozzi C et al (2001) Mechanism of syncope in patients with isolated syncope and in patients with tilt-positive syncope. Circulation 104:1261–1267
69. Strickberger SA, Benson DW, Biaggioni I et al (2006) AHA/ACCF scientific statement on the evaluation of syncope. Circulation 113:316–327
70. Brignole M, Alboni P, Benditt DG et al (2004) Guidelines on management (diagnosis and treatment) of syncope-update 2004. Eur Heart J 25:2054–2072
71. Adamson PB, Magalski A, Braunschweig F et al (2003) Ongoing right ventricular hemodynamics in heart failure: clinical value of measurements derived from an implantable monitoring system. J Am Coll Cardiol 41:565–571
72. Reynolds DW, Bartelt N, Taepke R, Bennett TD (1995) Measurement of pulmonary artery diastolic pressure from the right ventricle. J Am Coll Cardiol 25:1176–1182
73. Stevenson LW, Perloff JK (1989) The limited reliability of physical signs for estimating hemodynamics in chronic heart failure. JAMA 261:884–888
74. Wilson JR, Hanamanthu S, Chomsky DB, Davis SF (1999) Relationship between exertional symptoms and functional capacity in patients with heart failure. J Am Coll Cardiol 33: 1943–1947
75. Bennett T, Kjellstrom B, Taepke R, Ryden L (2005) Development of implantable devices for continuous ambulatory monitoring of central hemodynamic values in heart failure patients. Pacing Clin Electrophysiol 28:573–584